#7

Office of the Secretary of Defense 5 USC Sec. 552
Chief, RDD, ESD, WHS and
Date: 19 Jul 2013 Authority: EO 13526
Declassify: X Deny in Full: _____
Declassify in Part: _____
Reason: _____
MDR: 12-M-3150

AD- 329067

SECURITY REMARKING REQUIREMENTS

DOD 5200.1-R DEC 78

REVIEW ON 28 FEB 82

Page determined to be Unclassified
Reviewed Chief, RDD, WHS
IAW EO 13526, Section 3.5
Date: JUL 19 2013

5.3 (1).3

12-M-3150 R-7

~~CONFIDENTIAL~~

AD 329 067

Reproduced
by the

ARMED SERVICES TECHNICAL INFORMATION AGENCY
ARLINGTON HALL STATION
ARLINGTON 12, VIRGINIA

~~CONFIDENTIAL~~

NOTICE: When government or other drawings, specifications or other data are used for any purpose other than in connection with a definitely related government procurement operation, the U. S. Government thereby incurs no responsibility, nor any obligation whatsoever; and the fact that the Government may have formulated, furnished, or in any way supplied the said drawings, specifications, or other data is not to be regarded by implication or otherwise as in any manner licensing the holder or any other person or corporation, or conveying any rights or permission to manufacture, use or sell any patented invention that may in any way be related thereto.

329 067

General Mills

THE GENERAL MILLS ELECTRONICS GROUP

[redacted]

February 23, 1962

[redacted]

This document consists of 113 pages and is number 22 of 35 copies, series A, and the following — attachments.

SIXTH QUARTERLY PROGRESS REPORT ON DISSEMINATION OF SOLID AND LIQUID BW AGENTS

(Unclassified Title)

[redacted]

For Period September 4 - December 4, 1961
Contract No. DA-18-064-CML-2745

Prepared for:

U.S. Army Biological Laboratories
Fort Detrick, Maryland

Submitted by: G. R. Whitnah
Project Manager

Report No. 2264
Project No. 82408

Approved by: S. P. Jones
Manager, Materials and Mechanics Research

Research and Development
2003 East Hennepin Avenue
Minneapolis 13, Minnesota

[redacted]

ASTIA AVAILABILITY NOTICE

Qualified requestors may obtain copies of this document form ASTIA.

Foreign announcement and dissemination of this document by ASTIA is limited.

[redacted]

[redacted]

ABSTRACT

This Sixth Quarterly Progress Report covers the results of continued investigation of the many technical problems involved in the dissemination of solid BW agents and the effort devoted to the design and fabrication of a liquid BW agent disseminating store for use as a weapon on high speed, low-flying aircraft.

Progress on the theoretical studies of powder mechanics are outlined. The distribution of energy during the process of compaction of a finely divided solid is discussed. New experimental devices for these studies are described.

Experimental measurements of the shear strength of powders are reported. Of particular interest is the finding that an exponential relationship exists between shear strength and the bulk density. Data relative to the feeding of pre-compacted powders in piston-cylinder systems are reported.

Results are given covering experiments on the loss of viability produced by exposing dry biological aerosols to heated airstreams. The simulants Bg and Sm were exposed to temperatures in the range of 30°C to 130°C.

The findings of additional experimental studies of deagglomeration by slipstream energy are reported. The current emphasis is on assessment of the loss in effectiveness due to agglomeration.

Progress on feeding systems for dry agents is reported. A full-scale laboratory model of the feeding system for an airborne disseminator is described, and future test plans are outlined.

The approach to be used in designing the blow-down wind tunnel apparatus for future dissemination experiments at Fort Detrick is discussed. The principal operating parameters of this system are given.

Progress on the design and fabrication of the liquid agent disseminating store is reported. The main considerations in establishing the design are outlined and the status of this part of the project is summarized.

Additional findings of the systems analysis effort are reported. Flow rates (versus down-wind distance) required for a fixed infection probability were determined using the solid agents LE and N.

TABLE OF CONTENTS

Section	Title	Page
1.	INTRODUCTION	1-1
2.	THEORETICAL STUDY OF THE MECHANICS OF PARTICULATE MATERIALS	2-1
2.1	Theoretical Studies of the Process of Compaction for Dry Powders	2-1
2.2	Fundamental Compaction Experiments	2-2
2.2.1	Piston-Cylinder Compaction Experiment	2-2
2.2.2	Hydrostatic Compaction Experiment	2-3
2.2.3	Measurement of Energy Dissipation during Compaction	2-6
2.3	Experimental Studies on the Work of Compaction	2-7
3.	EXPERIMENTS ON THE CHARACTERISTICS OF POWDERS	3-1
3.1	Shear Strength of Powders as a Function of Compressive Stress	3-1
3.2	Shear Strength as a Function of Bulk Density	3-6
3.3	Piston-Cylinder Experiments	3-13
3.4	Experiments with a Laboratory Screw Feeder	3-19
3.4.1	Experimental Apparatus	3-20
3.4.2	Experimental Technique	3-23
3.4.3	Experimental Results	3-25
4.	EFFECT OF ELEVATED AIRSTREAM TEMPERATURES ON THE VIABILITY OF DRY AEROSOLS OF B. GLOBIGII AND S. MARCESCENS	4-1
4.1	Modification in Equipment and Techniques	4-1
4.2	Reproducibility of Results	4-2
4.3	Viability of Dry Aerosols of Bg and Sm	4-4
4.4	Effect of Compaction on the Viability of S. marcescens	4-7

TABLE OF CONTENTS (Continued)

Section	Title	Page
5.	DISSEMINATION AND DEAGGLOMERATION STUDIES	5-1
5.1	Introduction	5-1
5.2	Pneumatic Disseminator	5-2
5.3	Sm Dissemination – Small Scale Agglomerate Study	5-6
5.4	Sm Dissemination – Large Scale Agglomerate Study	5-14
6.	EXPERIMENTAL DRY-AGENT DISSEMINATOR	6-1
6.1	Description of Experimental Dry-Agent Disseminator	6-1
6.2	Test Stand and Auxiliary Equipment	6-8
6.3	Test Plans	6-10
7.	APPARATUS TO BE FURNISHED FOR DISSEMINATOR EXPERIMENTS AT FORT DETRICK	7-1
7.1	Safety	7-1
7.2	Air Supply for the Wind Tunnel	7-2
7.3	Heat Exchanger	7-3
7.4	Stilling Chamber and Filter	7-3
7.5	Nozzle and Test Section	7-4
8.	PROGRESS ON THE LIQUID DISSEMINATING STORE	8-1
8.1	Design Effort	8-1
8.1.1	Design of Tank Assembly	8-1
8.1.2	Design of the Fluid Handling System	8-2
8.1.3	Design of the Electrical System	8-3
8.1.4	Design of the Booms and Boom Actuator	8-4
8.2	Purchasing and Fabrication of Parts	8-5
9.	SYSTEMS STUDY	9-1
10.	SUMMARY AND CONCLUSIONS	10-1
11.	REFERENCES	11-1

LIST OF ILLUSTRATIONS

Figure	Title	Page
2.1	Piston-Cylinder Apparatus for Measuring Work of Compaction	2-4
2.2	Apparatus for Measuring Work for Compaction under Hydrostatic Loading	2-5
2.3	Work of Compaction per Gram versus Reciprocal Bulk Density for Several Powders	2-8
3.1	Shear Strength as a Function of Compressive Load for Bg Powder	3-3
3.2	Shear Strength versus Moisture Content of Two Powders at a Constant Compressive Load (15×10^3 dynes/cm^2)	3-4
3.3	Shear Strength of Talc as a Function of Compressive Stress	3-5
3.4	Shear Strength of Cornstarch as a Function of Compressive Stress	3-7
3.5	Apparatus for Determining Shear Strength versus Bulk Density	3-8
3.6	Shear Strength of Talc Powder as a Function of Bulk Density	3-11
3.7	Semi-Log Plot of Shear Strength versus Bulk Density for Talc Powder	3-12
3.8	Piston-Cylinder Device	3-15
3.9	Piston-Cylinder Results on Talc #18	3-16
3.10	Piston-Cylinder Results on Cornstarch	3-17
3.11	Piston-Cylinder Results on Bg (Uncompacted)	3-18
3.12	The Screw Feeder	3-20
3.13	Experimental Set-Up for Torque and Output Measurements of Screw Feeder	3-22

LIST OF ILLUSTRATIONS (Continued)

Figure	Title	Page
3.14	Screw Feeder Torque and Output Data for Cornstarch, Polyvinyl Alcohol and Talc Powder	3-26
3.15	Screw Feeder Troque and Output Data for Sm, Bg, and Saccharin Powders	3-27
4.1	Viability of Dry Aerosols of B. globigii Spores and S. marcescens in Elevated Air Temperatures	4-6
5.1	Mechanical-Pneumatic Disseminator Model	5-3
5.2	High Velocity Sampling Probe and Secondary Filtration System	5-7
5.3	Photomicrograph of Filter Samples of Sm Aerosol	5-9
5.4	Percentage of Sm Aerosol Particles (by number) consisting of Agglomerates in the 1 to 5-Micron and 5 to 20-Micron Ranges (Wind tunnel Mach number 0.5; sampling position - 0.63 cm below tunnel top wall)	5-10
5.5	Particle Size Distribution of Sm Aerosol on a Number Basis	5-12
5.6	Loss in Effectiveness of 1 to 5-Micron Sm Particles Due to Small Scale Agglomeration	5-15
5.7	Wind Tunnel Full-Flow Impactor	5-16
5.8	Photomicrographs of Impactor Sample (Sm)	5-18
5.9	Mass of Sm Collected on Impactor as Compared to Amount Disseminated (Wind Tunnel Mach Number 0.5)	5-19
6.1	Experimental Dry-Agent Disseminator for Laboratory Design Studies	6-2
6.2	Drive End of Disseminator	6-4
6.3	Disaggregator Removed from Center Section	6-5
6.4	Disaggregator Positioned in Center Section	6-6

LIST OF ILLUSTRATIONS (Continued)

Figure	Title	Page
6.5	Piston and Drive Screw in Cylinder	6-7
6.6	Adapter with Discharge Orifices	6-9
9.1	A Typical Curve for Probability of Infection versus Down-Wind Distance	9-4
9.2	A Typical Curve for Flow Rate versus Down-Wind Distance (x)	9-5
9.3	Flow Rate versus Down-Wind Distance for Agent N for "Average" Weather and h_a = 55 feet	9-6
9.4	Flow Rate versus Down-Wind Distance for Agent N for "Good" Weather and h_a = 55 feet	9-7
9.5	Flow Rate versus Down-Wind Distance for Agent N for "Average" Weather and h_a = 100 feet	9-8
9.6	Flow Rate versus Down-Wind Distance for Agent N for "Good" Weather and h_a = 100 feet	9-9
9.7	Flow Rate versus Down-Wind Distance for Agent LE for "Average" Weather and h_a = 55 feet	9-10
9.8	Flow Rate versus Down-Wind Distance for Agent LE for "Good" Weather and h_a = 55 feet (and 100 feet)	9-11

LIST OF TABLES

Number	Title	Page
3.1	Moisture Content of Bg and Sm at Various Relative Humidities	3-2
3.2	Shear Strength of Talc Powder Compressed to Different Bulk Densities	3-13
3.3	Torque Required to Move Various Powders through Laboratory Screw Feeder	3-24
3.4	Relative Ranking of Powders According to Screw Feeder Parameters	3-30
4.1	Reproducibility of Flow-Splitting Device in Elevated Airstream Temperature Apparatus	4-3
4.2	Viability of Dry Aerosols of Bg at 125°C for 1.68 Seconds (Bg from Lot No. X-12 Aerosolized with DeVilbiss Generator)	4-5
4.3	Viability of Dry Aerosols of Sm at Various Exposures (Sm from Pool #7 Aerosolized by Explosion)	4-5
4.4	Effect of Compression on Viability of Sm Powder (Sm from Pool #7)	4-8
5.1	Small-Scale Agglomeration of Sm Simulant Disseminated in Mach Number 0.5 Airstream with Pneumatic System	5-11
5.2	Description of Agglomerates in the 5 to 20-Micron Range	5-13
9.1	Nomenclature	9-1

1. INTRODUCTION

This is the Sixth Quarterly Progress Report on Contract No. DA-18-064-CML-2745 which deals with the dissemination of solid and liquid BW agents.

During this reporting period, work was continued on Phase II of the project, and Phase III, which covers an interim two-month continuation of the effort, was initiated.

This report covers progress on the theoretical and experimental studies of the characteristics of finely divided solids which are being conducted on a continuing basis throughout this program to provide data pertinent to the design and development of disseminators. Progress on the design and fabrication of a liquid-agent disseminating store is also summarized. Additional areas of investigation, closely related to the future design of a dry-agent disseminating store, are also covered. These are the wind tunnel studies of deagglomeration by aerodynamic breakup, the investigation of feeding and metering concepts and the systems studies.

2. THEORETICAL STUDY OF THE MECHANICS OF PARTICULATE MATERIALS

Theoretical studies during this reporting period have been primarily concerned with the energy of compaction of dry powders. On careful examination, the compaction process is found to be very complex, even when viewed as a macroscopic phenomenon. Before a rational theory of compaction can be developed, it is necessary to construct a model for powder behavior which is capable of describing the general properties of compacted powders. A discussion of these preliminary theoretical considerations is presented herein, together with new experimental data on the work of compaction for several test powders.

2.1 Theoretical Studies of the Process of Compaction for Dry Powders

When a powder is compacted, the work done on the powder may appear in three forms: 1) an increase in potential energy associated with interparticle bonds, 2) stored elastic energy in the bulk powder, and 3) thermal energy which is dissipated during the process. The first two forms of energy are reversible, whereas the latter is not recoverable. If the stresses applied to the powder in the course of compaction are removed, the elastic energy stored in the powder will be recovered externally, leaving only the potential energy increment permanently stored in the powder in its compacted state. It is reasonable to assume that the potential energy due to interparticle bonds depends principally on the configuration of the particle making up the powder aggregate; i.e., on the number of particle contacts in a given mass of powder. Furthermore, the bulk physical properties of a compacted powder will depend upon the interparticle bond energies.

It is apparent that several fundamental factors must be considered in the compaction process for a given powder. Suppose a powder of initial bulk density ρ_0 is compacted to a density ρ_1 by the expenditure of work W.

The work done on the powder can be expressed in terms of the work done by applied surface stresses during the compaction process. The following questions arise in regard to this process:

1) What fraction of the work W appears as elastic energy stored in the powder, with the stresses applied to reach the final compaction state maintained after compaction?

2) What fraction of W represents the increase in potential energy of interparticle bonds?

3) What is the process of energy transfer from the elastic component (which is macroscopically reversible) to the macroscopically irreversible potential energy and dissipative components during compaction?

4) How do the above relationships depend upon the path, i.e., the manner of application of stresses during compaction?

In order to resolve these questions, several interesting experiments are being devised as described below. These experiments should furnish an insight into the mechanism of compaction which is required in formulating an analytical theory of compactible powders.

2.2 Fundamental Compaction Experiments

Three types of experiments relating to the compaction of dry powders are required for a better understanding of the compaction process. The first two experiments are concerned with the work (or energy) required to compact a given mass of powder between two density states. The third experiment would measure the fraction of the total compaction energy which is dissipated as heat.

2.2.1 Piston-Cylinder Compaction Experiment

The piston-cylinder experiment is designed to permit measurement of the total energy W absorbed by a powder during compaction, as well as the fraction of this energy which is stored in recoverable form, i.e., elastically.

The detailed structure of the compaction process would also be explored with this apparatus, that is, the way in which the work done on the powder is absorbed. It is anticipated that the transfer of energy from the elastic component by internal dissipation or through an increase in the potential energy of particle contacts will be discontinuous. This behavior should be observable in tests with a small powder sample if the deformation of the powder is measured with a sensitive apparatus.

An improved version of the piston-cylinder compaction apparatus used in previous work[1] is being designed for this investigation. The device, shown schematically in Figure 2.1, will employ a strain gage transducer for measurement of the stress applied to the powder. A sensitive differential transformer will be used to measure displacements of the piston. The applied stress and resulting displacement will be recorded simultaneously during the experiment.

2.2.2 Hydrostatic Compaction Experiment

The piston-cylinder compaction experiment will provide numerical data on compaction energy as a function of density under the conditions of the test, that is, subject to the constraints and loading conditions imposed by the apparatus. Since the results obtained may depend to a considerable degree on the apparatus used, it is desirable to measure the compaction energy under conditions where no constraint is imposed by the apparatus. This can be done with the hydrostatic compaction apparatus shown in Figure 2.2. In this test the powder sample, which is sealed within a thin water-tight membrane, is placed in a pressure chamber. A hydrostatic pressure is then gradually applied and changes in volume of the sample noted. The work done in compacting the sample is $\int p dV$, where p is the chamber pressure and V is the chamber volume. It will be necessary to vent the powder sample as shown in the figure.

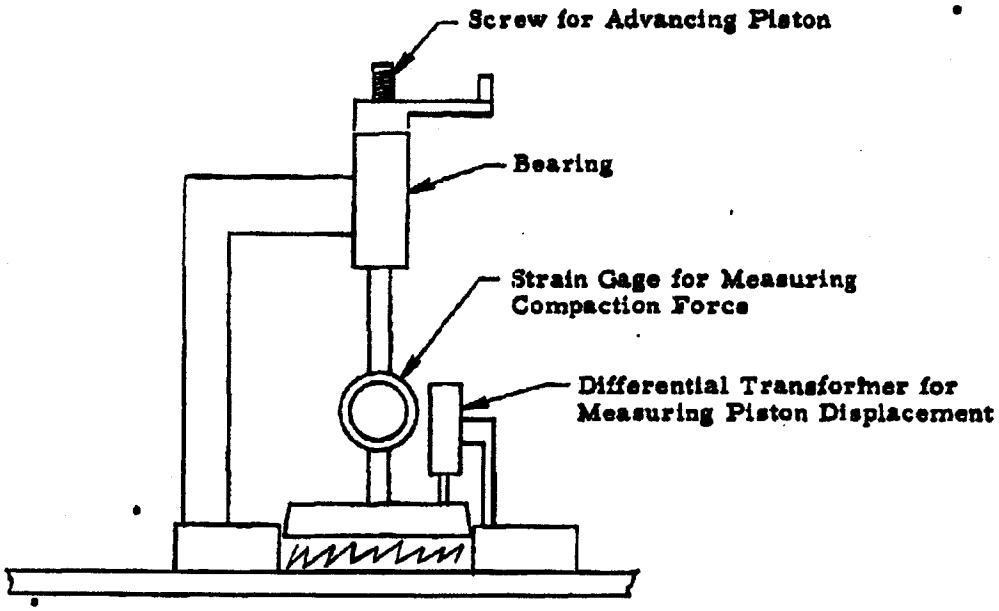

Figure 2.1 Piston-Cylinder Apparatus for Measuring Work of Compaction

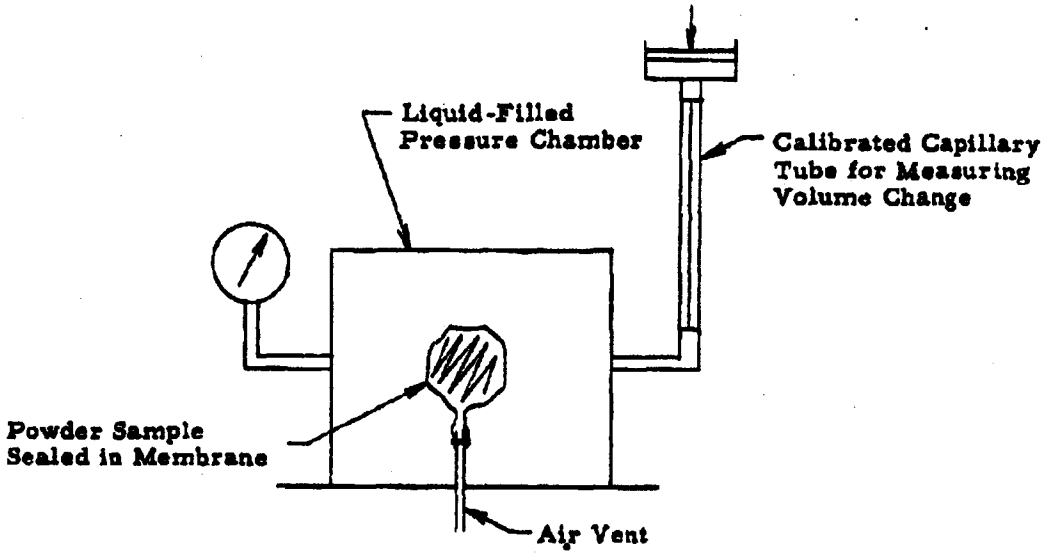

Figure 2.2 Apparatus for Measuring Work for Compaction under Hydrostatic Loading

It is quite possible that the energy of compaction obtained from the hydrostatic compaction experiment will agree with results from the piston-cylinder test. In this case, the compaction energy-density relationship for a powder may be considered to be a fundamental of the property powder. This conclusion would be of great importance in the development of an analytical theory of powder mechanics.

2.2.3 Measurement of Energy Dissipation during Compaction

The energy dissipated as heat during the compaction process can be evaluated by directly measuring the temperature rise within the powder. It appears likely that most of the work done in compacting a loose powder will be dissipated by internal friction, at least in the initial stages of compaction. If the fraction of the applied work which is dissipated during compaction of a powder can be experimentally determined, important conclusions may be reached regarding the ease of deagglomerating the material, since the balance of the energy would be attributed to interparticle bond energies.

An attempt to measure energy dissipation within a powder undergoing compaction will be made using the piston-cylinder apparatus shown schematically in Figure 2.1. The temperature rise will be measured by using a thermopile having a large number of junctions in series within the powder, with intermediate junctions maintained at a fixed temperature outside the powder bed. Preliminary calculations indicate that the temperature rise corresponding to energy inputs of about 10^5 ergs/gram would be about 0.01°C (for talc, this energy input would yield a bulk density of about $\rho = 0.55$ g/cc). This estimate of the powder temperature rise assumes that all of the energy input is dissipated as heat and that the specific heat of the powder is about 0.25 cal/gram. It will of course be necessary to measure the specific heat of the powder in its compacted state in order to interpret the experimental results. Although this experiment will be rather difficult to perform with satisfactory accuracy, because of the very small energy involved in the compaction process, positive results will be of essential importance in the formulation of an analytical compaction theory.

Work is presently in progress in designing apparatus and developing experimental procedures for these compaction experiments.

2.3 Experimental Studies on the Work of Compaction

During this reporting period, the work of compaction was determined as a function of density for several powders, using the apparatus and experimental technique employed in earlier experiments with talc powder[1]. The results of these tests are shown in Figure 2.3 for the following powders: saccharin, Sm, corn starch and talc. Within the accuracy of the measurements, the net work of compaction (i.e., the total work done on the powder less the elastic energy stored in the powder) was found to be related to the bulk density by a relationship of the form: $W = C/\rho^n$, where W is the work in ergs/gm. The constants of the equation are given in the following table:

Powder	n	$C \times 10^{-5}$
Talc	4.37	9.75
Saccharin	3.80	10.5
Sm	6.95	56.8
Cornstarch	11.80	4.4

As pointed out in the above discussion (Section 2.2.2), these results may be influenced by the apparatus used for compaction of the powder. However, it appears possible that the power-law relationship between compaction work and bulk density may be valid for a number of powders.

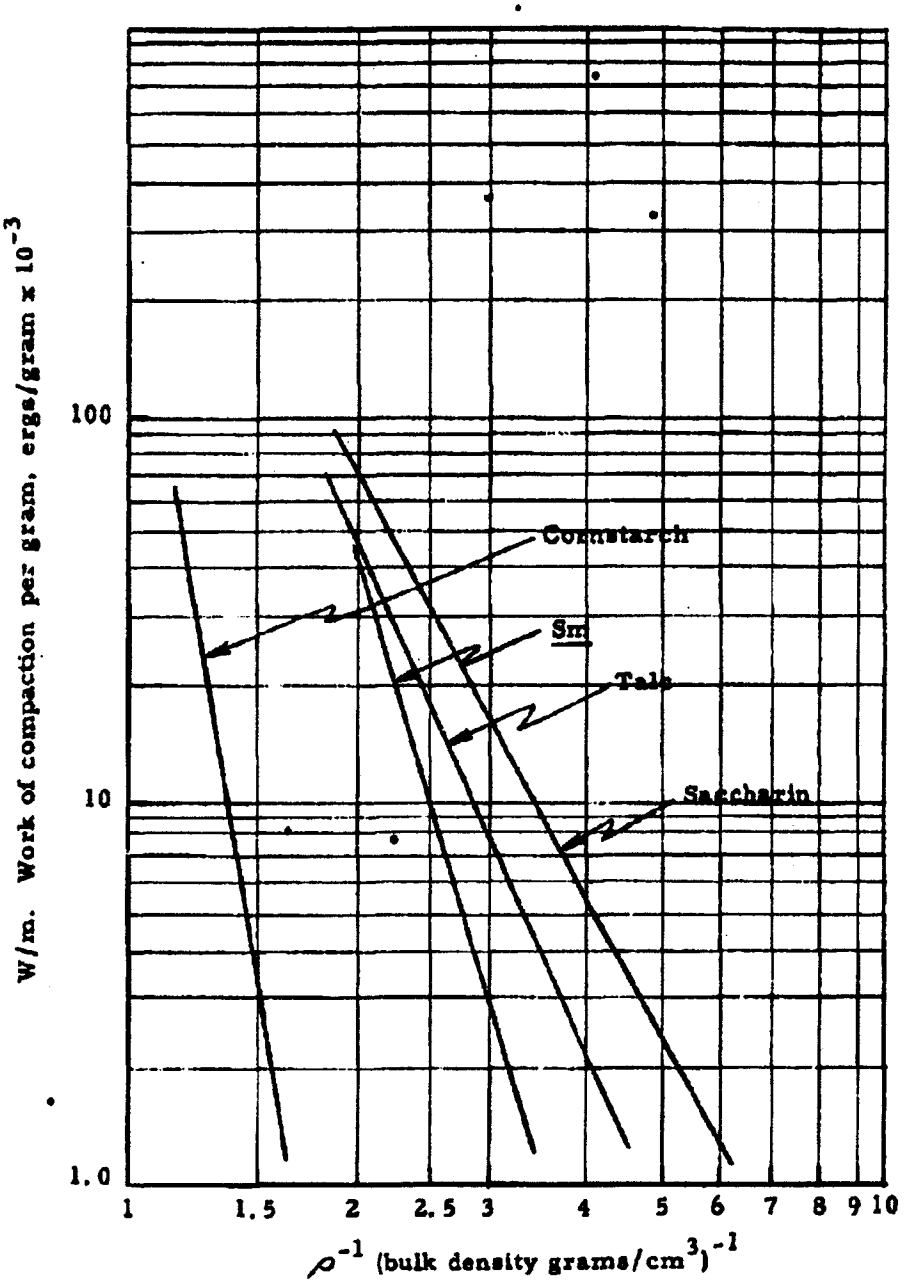

Figure 2.3 Work of Compaction per Gram versus Reciprocal Bulk Density for Several Powders

3. EXPERIMENTS ON THE CHARACTERISTICS OF POWDERS

In order to determine those fundamental properties of finely-divided dry powders which affect their feeding and handling characteristics, information is being obtained on the coefficient of friction of powders sliding against various materials, the bulk density of powders as a function of compressive load, and the shear strength of powder beds. These characteristics will then be correlated to the output and energy required to operate such powder feeding devices as piston and screw feeders.

3.1 Shear Strength of Powders as a Function of Compressive Stress

The shear strength of powders is being studied as one of the important factors to be considered in determining the energy required to operate a piston or screw feeder. When fine powder is discharged from a cylinder or a screw there is generally some powder remaining on the walls. Therefore, energy has been expended in shearing this powder from the mass of powder which was discharged.

The "sliding disc" method used to measure the shear strength of powders has been described in a previous report and results obtained on Sm, talc, and polyvinyl alcohol have been presented.[2] During the period covered by this report, shear strength measurements were made on Bg (Bacillus globigii) powder as a function of moisture content. These measurements were made in a controlled humidity chamber described in a previous report[2]. The humidity range of these tests was from < 1 percent to 60 percent relative humidity at 78°F. For each humidity where shear strength measurements were made, a sample of the powder was analyzed for moisture content according to the method of Flosdorf and Webster[3]. This method involves measuring weight loss upon heating for 22 to 24 hours at 50°C in a vacuum oven at 50 to 100 μ pressure. Table 3.1 shows the moisture content of two powders, Bg and Sm at various relative humidities.

Table 3.1 Moisture Content of Bg and Sm at Various Relative Humidities

Relative Humidity (% at 78°F)	Moisture Content of Bg Powder (%)	Moisture Content of Sm Powder (%)
1	2.4	2.8
15	5.0	3.4
30	7.3	5.3
45	11.6	11.7
60	14.8	17.7

Figure 3.1 shows the shear strength of Bg powder versus the compressive load for varying powder moisture content. It will be noted that the shear strength changes very little as the moisture content of the powder is increased from 2.4 percent to 11.6 percent. However, at 14.8 percent moisture content the shear strength definitely decreases. Figure 3.2 presents a comparison of the shear strength of two powders, Bg and Sm, for varying moisture content at a constant compressive load of 15×10^3 dynes/cm^2. The shear strength of Sm increases with increasing moisture content until it reaches a maximum value at a moisture content somewhere between 3.4 percent and 11.7 percent and then decreases with increasing moisture content. The shear strength of Bg powder remains relatively constant up to a moisture content of 11.6 percent and then decreases with increasing moisture content. Shear tests on talc powder were extended to higher compressive stresses during the present period. Extrapolation of the original shear strength data on talc agrees very well with the new data at higher compressive stresses. Both the original and new data are presented graphically in Figure 3.3. It is apparent that a linear relationship between shear strength and compressive stress can be used to represent the data obtained thus far.

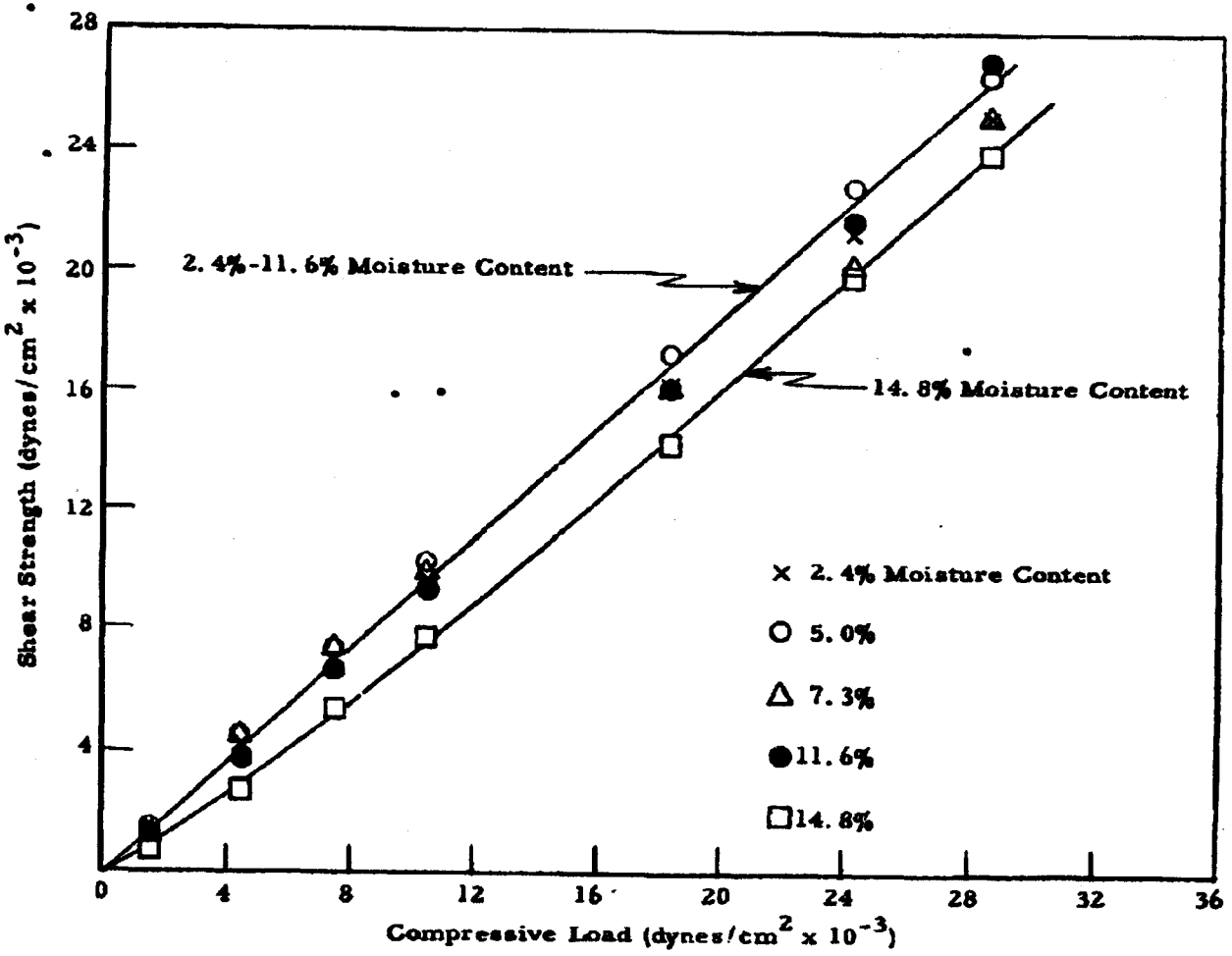

Figure 3.1 Shear Strength as a Function of Compressive Load for Bg Powder

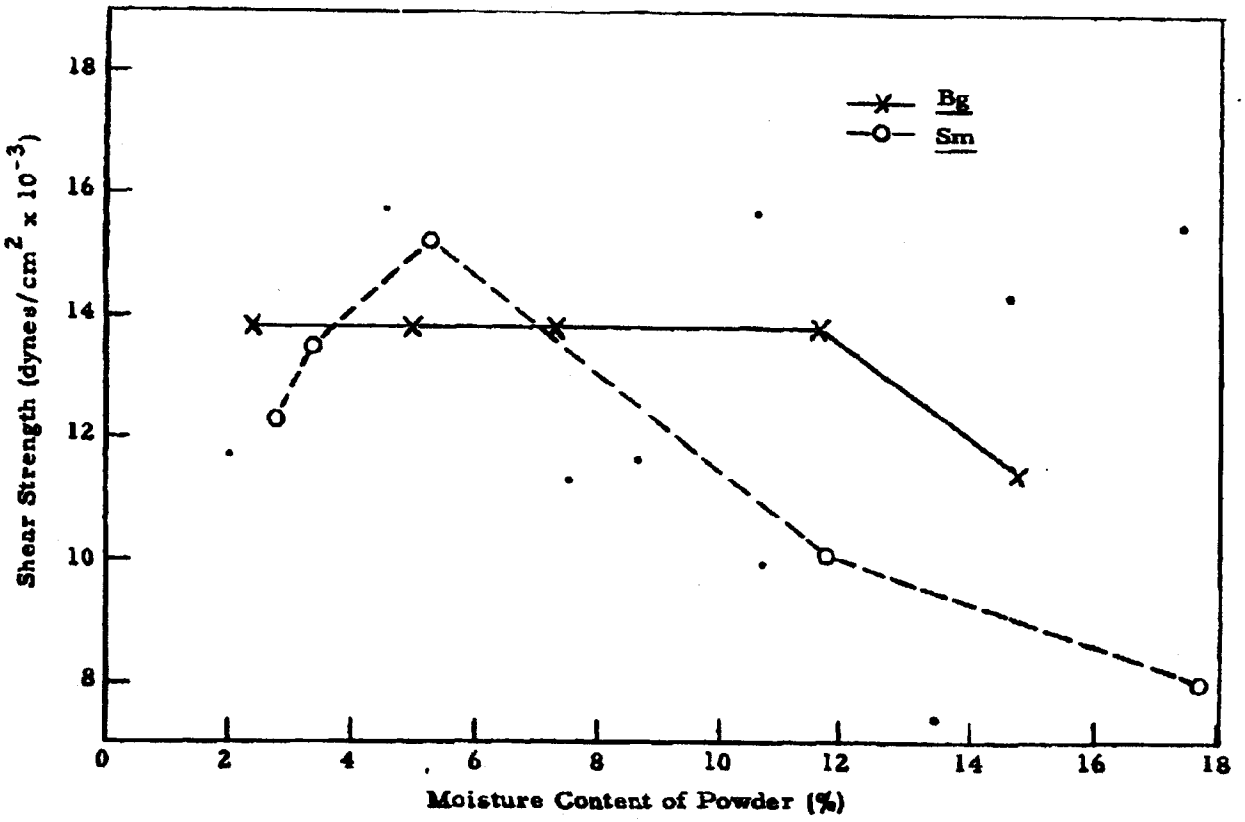

Figure 3.2 Shear Strength versus Moisture Content of Two Powders at a Constant Compressive Load (15×10^3 dynes/cm^2)

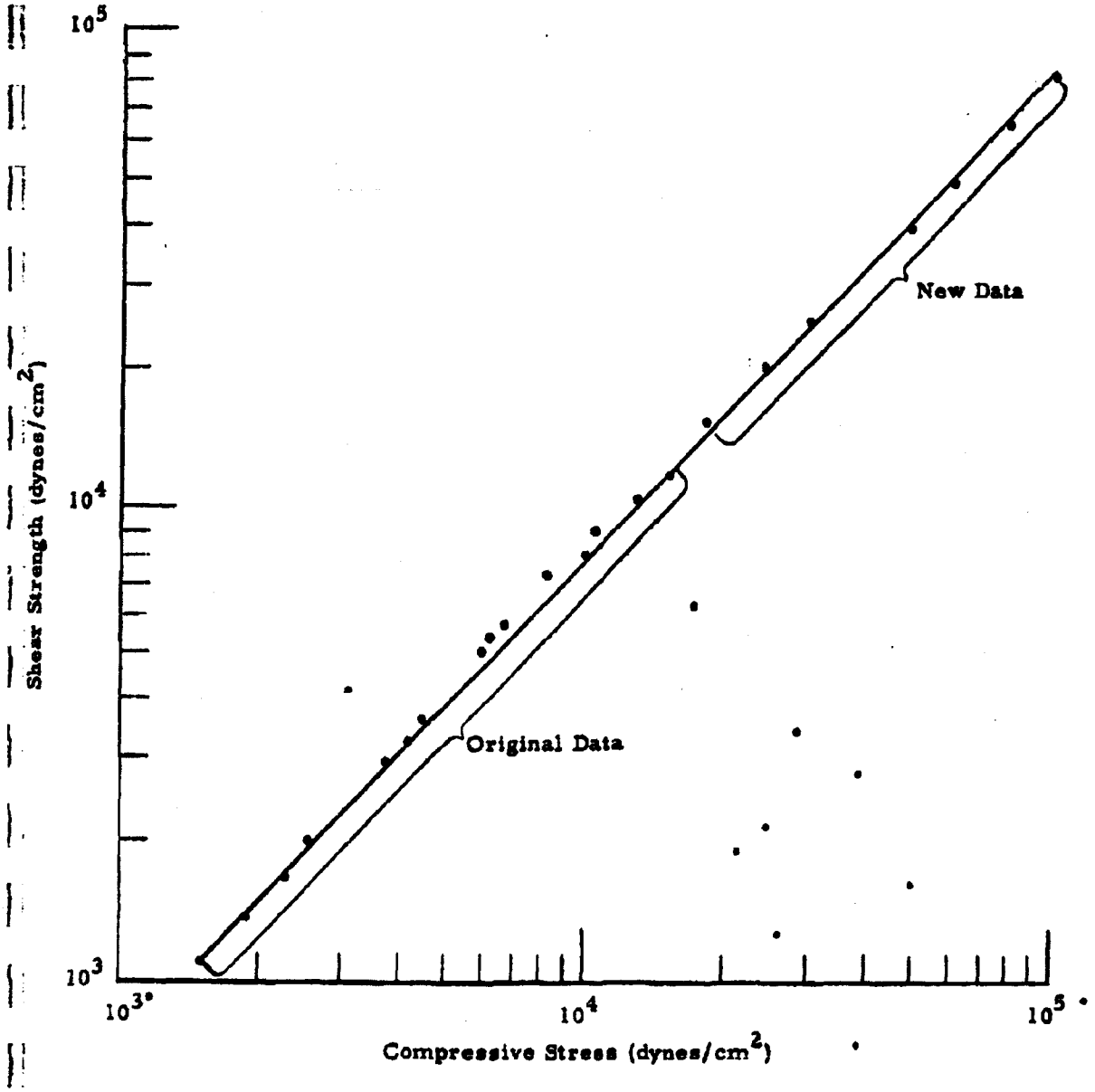

Figure 3.3 Shear Strength of Talc as a Function of Compressive Stress

Shear strength measurements on cornstarch as a function of compressive stress were initiated during this period. The data obtained to date are presented in Figure 3.4. Again, a linear relationship between shear strength and compressive stress was found in the region studied.

Future work will be directed at extending measurements on all powders to higher compressive loads, and auxiliary tests will be made to determine the bulk densities created by these compressive loads in order to correlate shear strength with bulk density for this particular test.

3.2 Shear Strength as a Function of Bulk Density

Previous tests on the shear strengths of powders were made by the "sliding disc" method. This method gives the shear strength of a thin layer of powder which is subjected to a known compressive stress before and during the application of a shearing force. Thus, one can find the shear strength as a function of compressive stress. The bulk density created by the compressive stress cannot be directly determined in this particular test. Because data concerning the shear strength as a function of bulk density are essential to this program, a new technique was explored for obtaining such information.

The apparatus shown in Figure 3.5 consists of three lengths of 1.37-inch I.D. aluminum tubing. Two pieces, 2-1/4 inches and 10 inches in length are held in concentric alignment by a piece of 90-degree angle aluminum, to which they are attached with epoxy resin. The angle aluminum is in turn attached to a small stand. These two pieces of tubing are spaced such that the gap between them is slightly greater than one-half inch. The third piece of tubing is one-half inch in length and slips easily into this gap. A small eyelet is attached to the outer surface of this ring.

The procedure in making a test is as follows: the ring is inserted in place, and small shims are inserted in the spaces between the ring and the tubes. The entire apparatus is placed on end, with the short sections

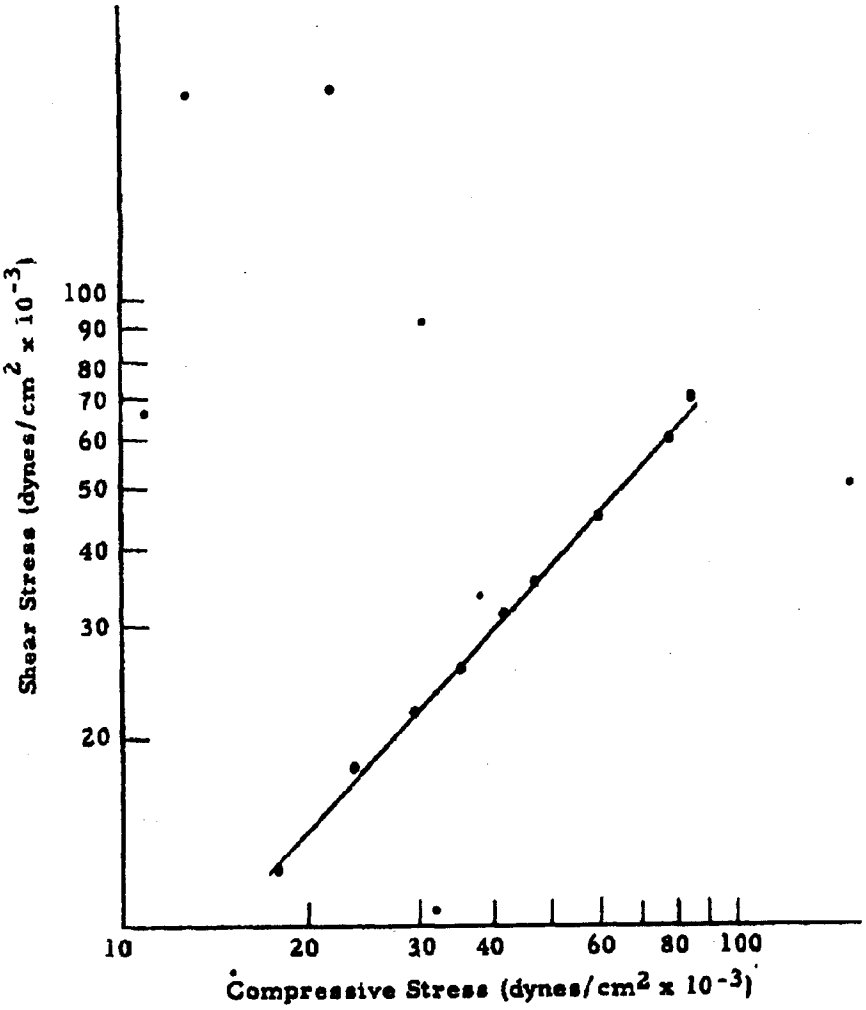

Figure 3.4 Shear Strength of Cornstarch as a Function of Compressive Stress

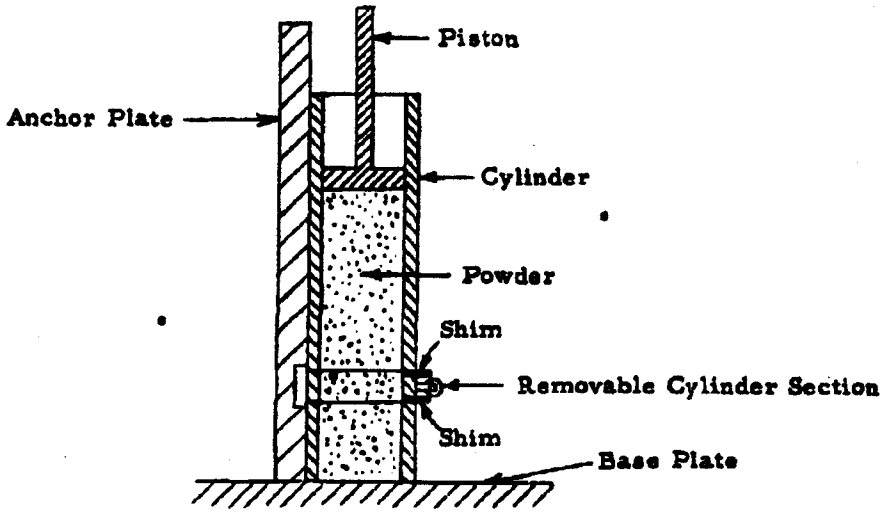

a. Compaction Process

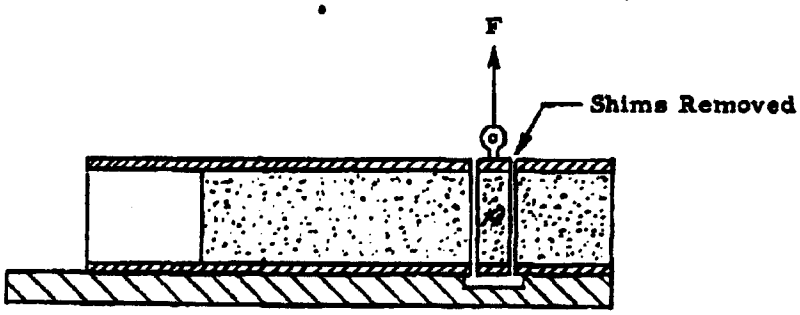

b. Shear Strength Measurement

Figure 3.5 Apparatus for Determining Shear Strength versus Bulk Density

nearest the bottom. The tube is then filled with powder, and the powder is compressed with a piston. The piston is removed, the tube is returned to a horizontal position, and the shims are removed. A force, measured with a strain gage transducer, is applied to the eyelet until the powder is sheared and the ring lifts. The ring and the powder within it are then weighed, and the average bulk density is calculated. The shearing force is the difference between the lifting force and the weight of ring and powder. The shear strength can now be calculated. Obviously, different bulk densities are obtained by using different amounts of powder and different compressive forces.

A study has been made of the manner in which local bulk density varies with distance along a plug of powder after compression in a tube.[4] It was found that for some powders there is a region near the bottom of the tube in which the local bulk density is essentially constant over relatively large distances. It is, of course, desirable that the bulk density at both faces of the ring be as nearly equal as possible in the present test method. With this in mind the apparatus was designed so as to locate the ring in this region.

It was found that such a flat region does not exist for talc, the powder which was used for the initial experiments. This does not present any real problem, however. The lifting force is given by

$$F = AS_1 + AS_2 \tag{3.1}$$

where A is the area of the shearing surface and S_1 and S_2 are the shear strengths at the two regions of shear where bulk density is ρ_1 and ρ_2. If S_1 and S_2 differ due to different values of ρ_1 and ρ_2, we can say

$$F = 2A\bar{S} \tag{3.2}$$

where:

$$\bar{S} = 1/2\,(S_1 + S_2) \qquad (3.3)$$

Thus, it is the average of the two shear strengths which is measured.

Within any small interval $\rho_1 \leq \rho \leq \rho_2$, it is assumed that the shear strength $S(\rho)$ is a linear function of ρ:

$$S(\rho) \approx K\rho \quad , \qquad (3.4)$$

Thus, the shear strength at the center of the interval can be approximated by the average of the shear strengths at the end points of the interval.

Also, the value obtained for the bulk density is the average bulk density throughout the entire ring. This closely approximates the average of the local bulk densities at the end points. Therefore, one can then say that the average shear strength as measured corresponds to the average bulk density as measured, provided the difference between the local bulk densities at the shearing faces is not too great.

The apparatus was constructed and tests were made to determine if binding between the ring and tube would be a problem. This effect was found to be negligible.

A set of preliminary measurements were then made on talc and the results are presented in Table 3.2 and Figure 3.6. When plotted on semi-log paper (Figure 3.7) a straight line results. This indicates a function of the form:

$$S(\rho) = K_1 e^{K_2 \rho} \qquad (3.5)$$

or, in other words, the shear strength is an exponential function of the bulk density.

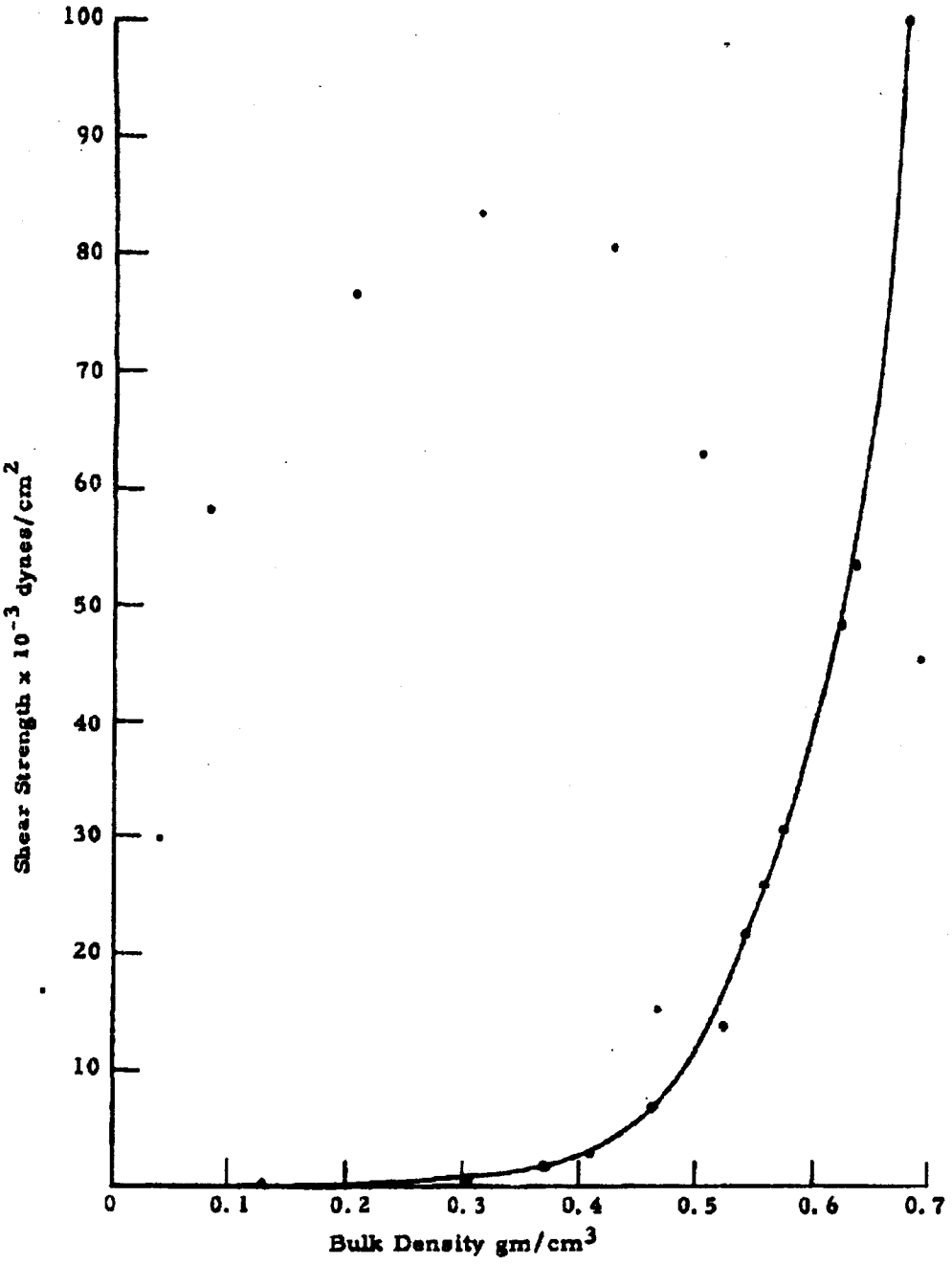

Figure 3.6 Shear Strength of Talc Powder as a Function of Bulk Density

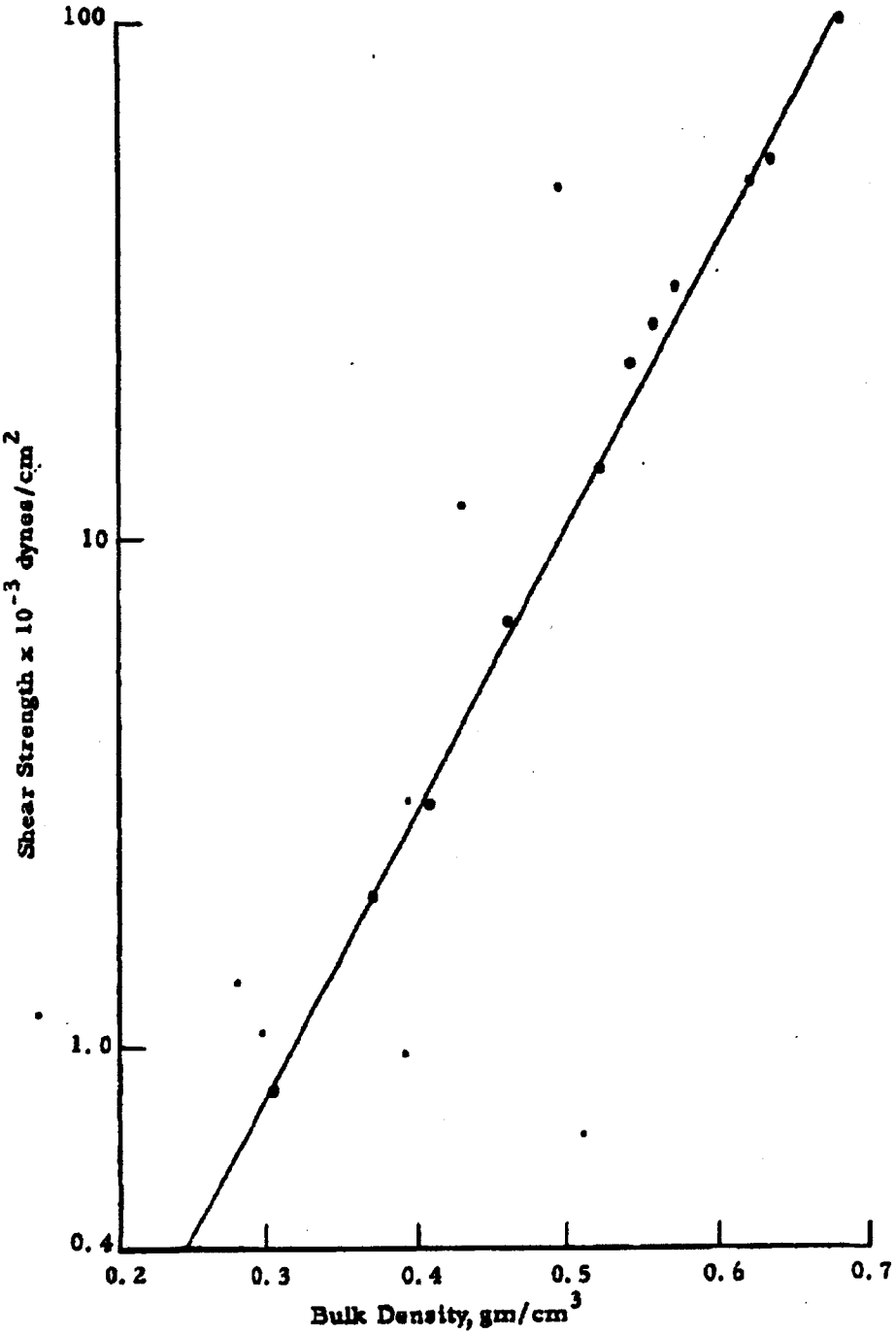

Figure 3.7 Semi-Log Plot of Shear Strength versus Bulk Density for Talc Powder

Further analysis of this technique is planned during the next quarter to determine whether this particular test is measuring pure shear strength, or a combination of shear stress plus force of compaction during lifting of the ring.

Table 3.2 Shear Strength of Talc Powder Compressed to Different Bulk Densities

Lifting Force (dynes x 10^{-3})	Shearing Force (dynes x 10^{-3})	Shear Strength (dynes/cm^2 x 10^{-3})	Bulk Density (gm/cm^3)
16.7	7.30	0.404	0.129
25.0	15.1	0.833	0.304
46.3	35.7	1.97	0.371
66.0	54.9	3.03	0.408
135	124	6.81	0.463
259	248	13.6	0.525
406	393	21.7	0.544
482	469	25.9	0.560
565	552	30.5	0.576
874	860	48.2	0.625
982	968	53.4	0.637
1,830	1,820	100.0	0.686

3.3 Piston-Cylinder Experiments

Since the last reporting period, the piston-cylinder apparatus has been modified by incorporating a dynamometer to measure the applied force and a Brush oscillograph to record the force. A further modification of the technique was the use of compacted plugs of powder. Information has been obtained on the force required to move powder plugs which have been compacted to a uniform density. Uniform density throughout the length of the plug was achieved by a lamination process in which small amounts of powder were added to and compacted in the cylinder in a stepwise fashion until

the desired plug length was obtained. Previous data were limited to powder columns which were uncompacted prior to the application of the resistive force (F_R). During the present reporting period, a comparison was made of the force required to move both uniformly compacted and uncompacted plugs of talc, cornstarch, and Bg powder through a cylinder.

To review briefly the test procedure, reference is made to Figure 3.8. The applied force (F_A) necessary to initiate movement of the powder plug of length L is determined when the plug is subjected to a resistive force (F_R). In the case of compacted plugs of uniform density, experiments were performed in which the resistive force (F_R) was varied from 4 percent to 100 percent of the force which was used in forming the laminated plug.

The cylinder used for the current experiments was made of stainless steel with an I.D. of 1.5 inches and a surface roughness of 10 to 15 microinches.

For the uncompacted powder plugs, a plot of the ratio of the applied force to the resistive force (F_A/F_R) against the ratio of the final plug length to its diameter (L/D) yielded a straight line when plotted on semi-log paper (Figures 3.9, 3.10, and 3.11). Thus, in the uncompacted state, the behavior of talc, cornstarch, and Bg powders follows the relationship reported:[5]

$$F_A/F_R = e^{\frac{4\mu CL}{D}} \qquad (3.6)$$

When talc or cornstarch was laminated with a compressive force (F_C) to form a plug of uniform density and the movement was restricted with a reduced load (the resistive force, F_R) then the force required to move the plug (F_A) was identical to that required to move an uncompacted plug of the same length subjected to the same resistive force, provided that F_R was greater than some critical value (C). In other words, the results with

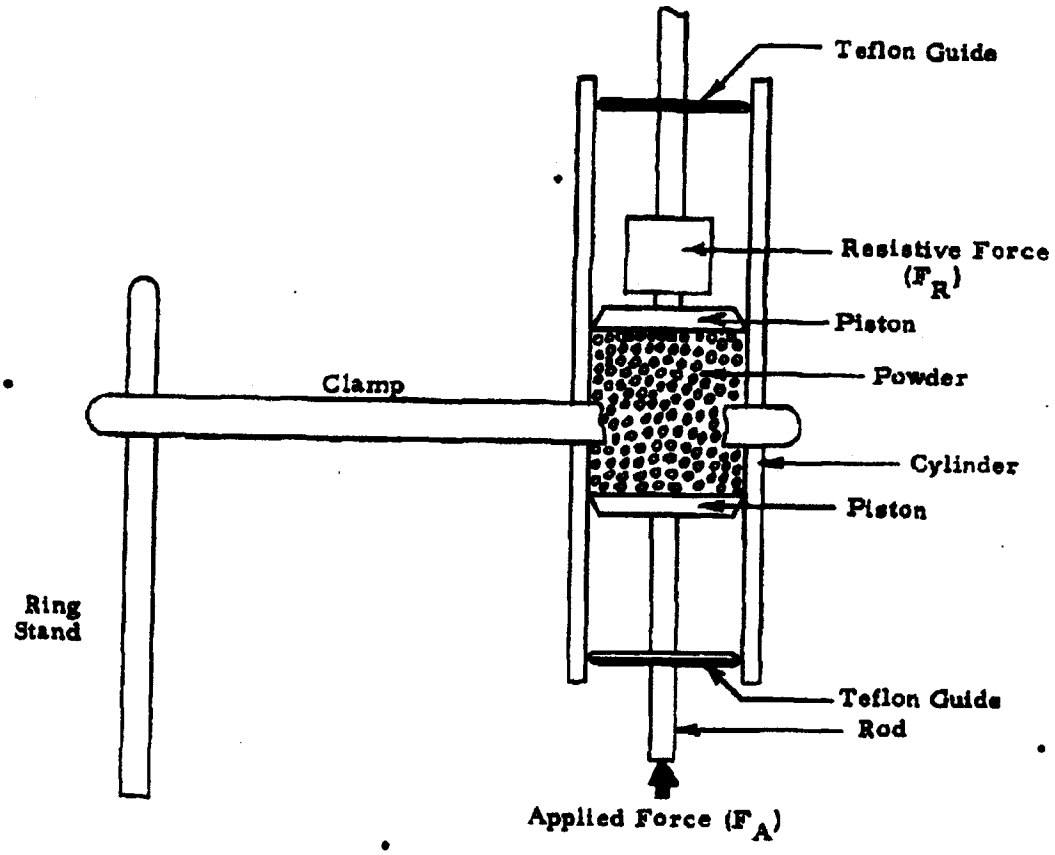

Figure 3.8 Piston-Cylinder Device

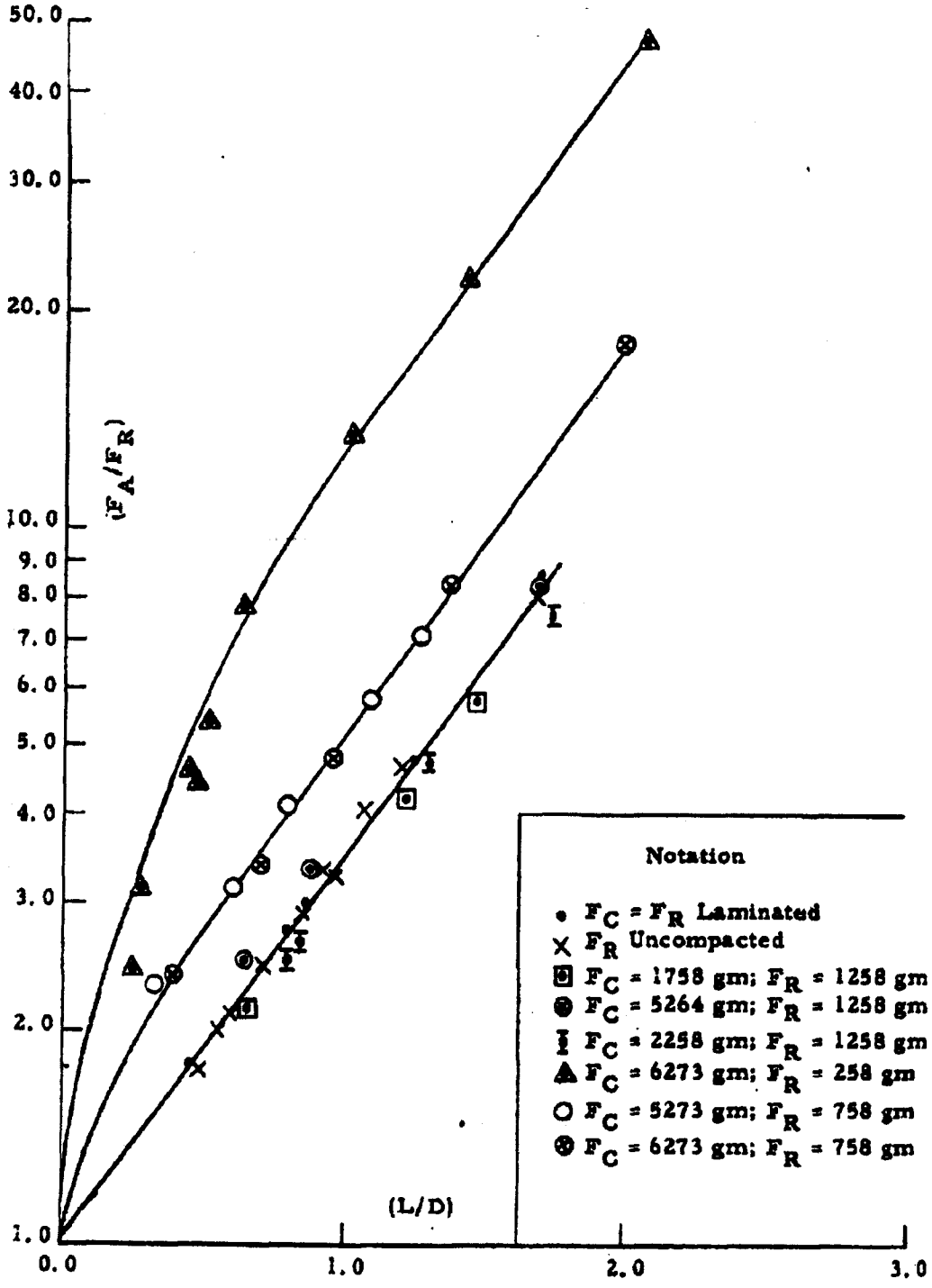

Figure 3.9 Piston-Cylinder Results on Talc #18

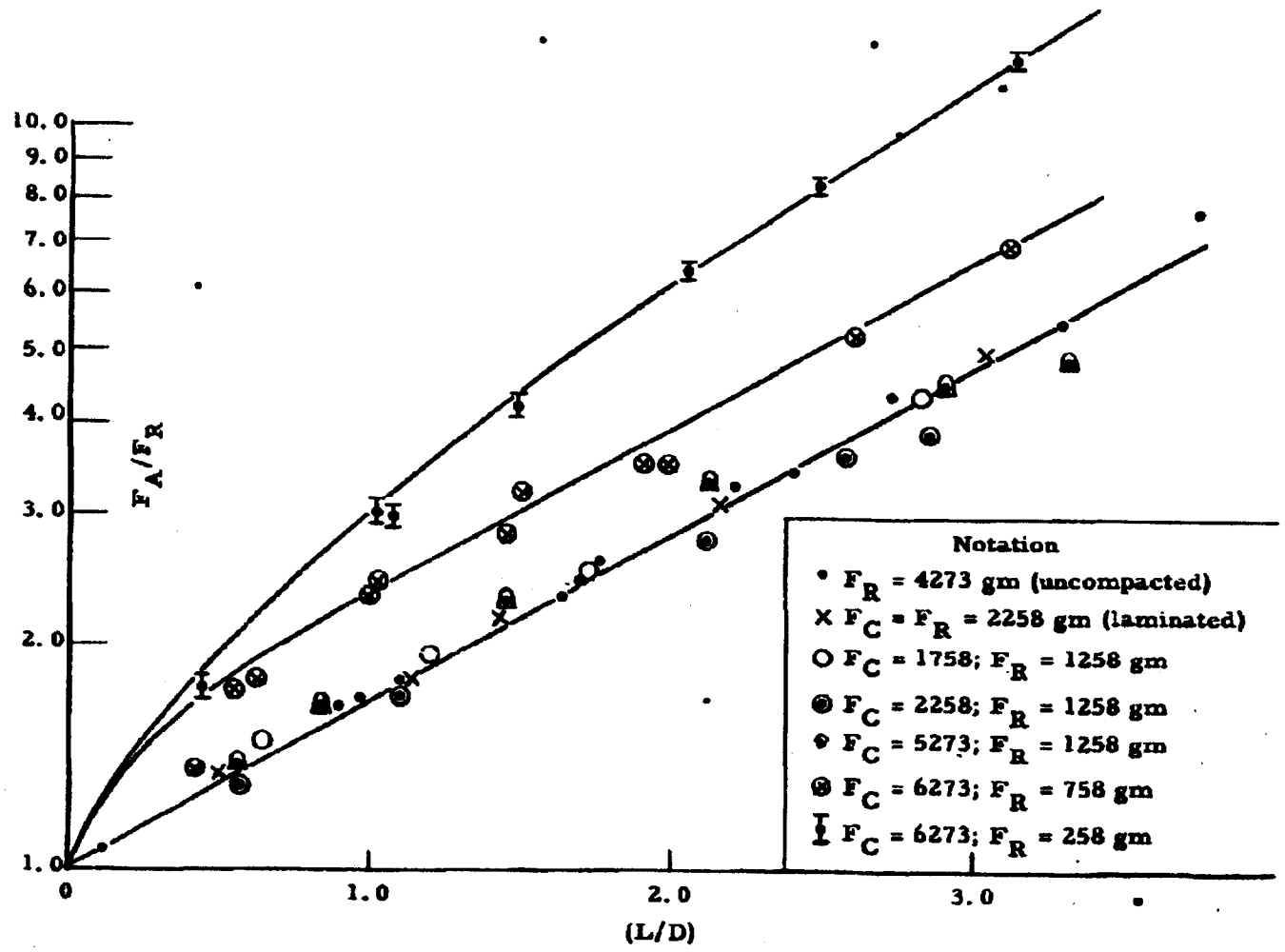

Figure 3.10 Piston-Cylinder Results on Cornstarch

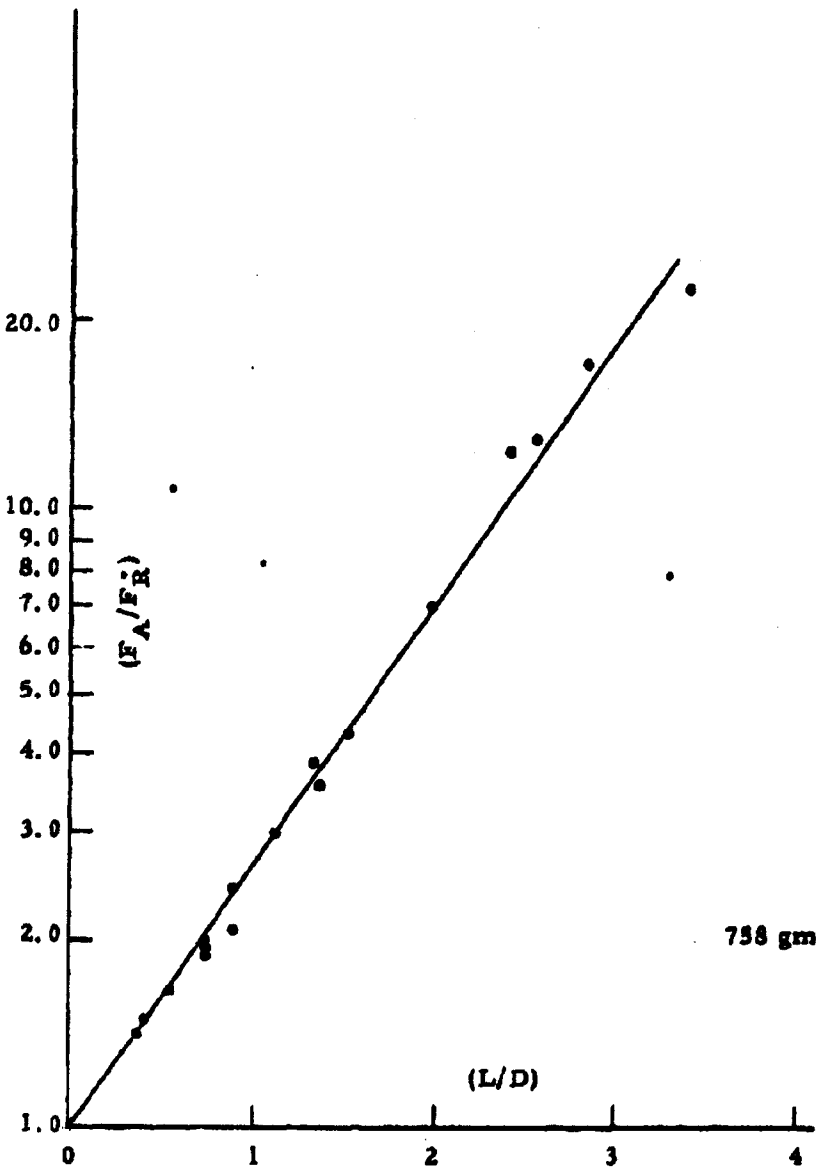

Figure 3.11 Piston-Cylinder Results on $\underline{B}g$ (Uncompacted)

plugs of uniform density yielded the identical straight line upon making a semi-log plot of F_A/F_R versus L/D providing $C \leq F_R \leq F_C$. If the resistive force was less than the critical force, C, then a new curve was generated. Figures 3.9 and 3.10 which present the results for talc and cornstarch respectively illustrate this behavior. At small L/D the slope of the curves obtained when F_R is less than the critical force is greater than the slope of the straight line obtained when $C \leq F_R \leq F_C$. The slope increases as the difference between F_R and F_C becomes larger. However, at large L/D (1.5 to 3.0), the slope of the curves becomes approximately equal to that of the straight line. The exact value of the critical force, C, was not determined; however, it appears to be equal to approximately 20 percent of the laminating force, F_C, used in forming the plug of uniform density. The full significance of these findings has not been determined at this time. Further experiments will have to be performed before a conclusion can be reached.

Piston-cylinder tests on Bg powders were performed only with uncompacted plugs. The results obtained are presented in Figure 3.11. The value of the slope ($C\mu$) of the straight line obtained is 0.237 for Bg compared to 0.315 for talc and 0.134 for cornstarch.

3.4 Experiments with a Laboratory Screw Feeder

One of the techniques previously considered for feeding and metering dry powders is the screw feeder. Preliminary experiments were performed to determine the output of such a device as a function of advancement of the screw.[6] Results obtained indicated that the rotational speed would have to be programmed in order to achieve a constant output of powder. To further determine the feasibility of this system, experiments were made to determine the torque, both starting and maximum, required to operate such a feeder, and the efficiency of the feeder in terms of the percent of initial powder charge which is ejected.

Six powders were tested in a laboratory scale unit. The powders were Sm, Bg, talc 18, polyvinyl alcohol (PVA 72-51), saccharin and cornstarch. The cornstarch used was a commercial grade containing about 3 percent of tri-calcium phosphate additive to inhibit caking. An attempt was made to correlate the results obtained in the screw feeder with other physical properties of the powder tested.

3.4.1 Experimental Apparatus

The screw feeder (Figure 3.12) consisted of an aluminum cylinder 4.75 cm in diameter and 25.8 cm long. The screw, 4.4 cm in diameter and consisting of five turns, was made of steel. A volume of 351 cm^3 was available for the powder. The screw was mounted in two ball bearing races, resulting in a non-load torque which was found to be insignificant in comparison to the torque required under full load conditions.

A second aluminum cylinder was placed around the screw feeder. For convenience in loading, a slot 2 cm wide was cut the length of the feeder in the inner cylinder. A slot 4 cm wide, centered over the opening in the inner cylinder, was cut in the outer cylinder. The material cut from the outer cylinder was used as a cover for the feeder to prevent powder from being forced out of the feeder during operation.

To measure the efficiency of the screw feeder, a technique for weighing the powder forced out of the feeder during revolution of the screw was devised. The technique used consisted of two strain gages applied to each of 4 thin split rings fastened between a base plate and a metal pan (Figure 3.13). A paper insert was placed in the pan to catch the powder as it emerged from the feeder. The output of the full-bridge strain gage circuit was fed to a Sanborn 170 dual channel recorder. In this manner, a continuous record of the amount of powder that was ejected from the feeder during revolution of the screw was obtained

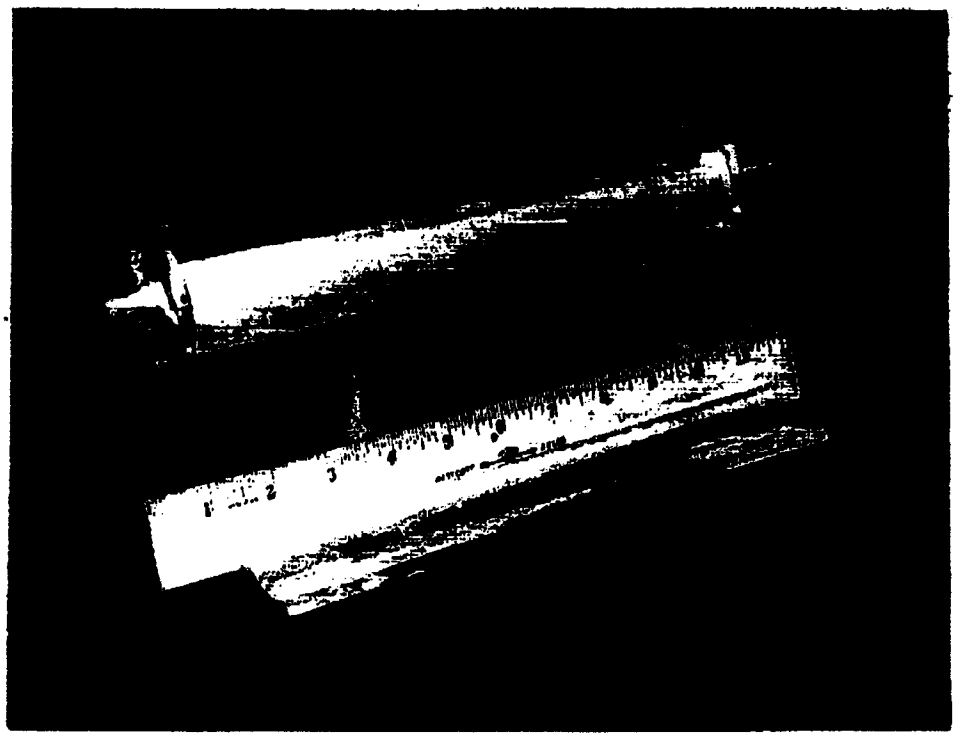

Screw Feeder Assembly

Helical Screw

Figure 3.18 Two Views of Screw Feeder

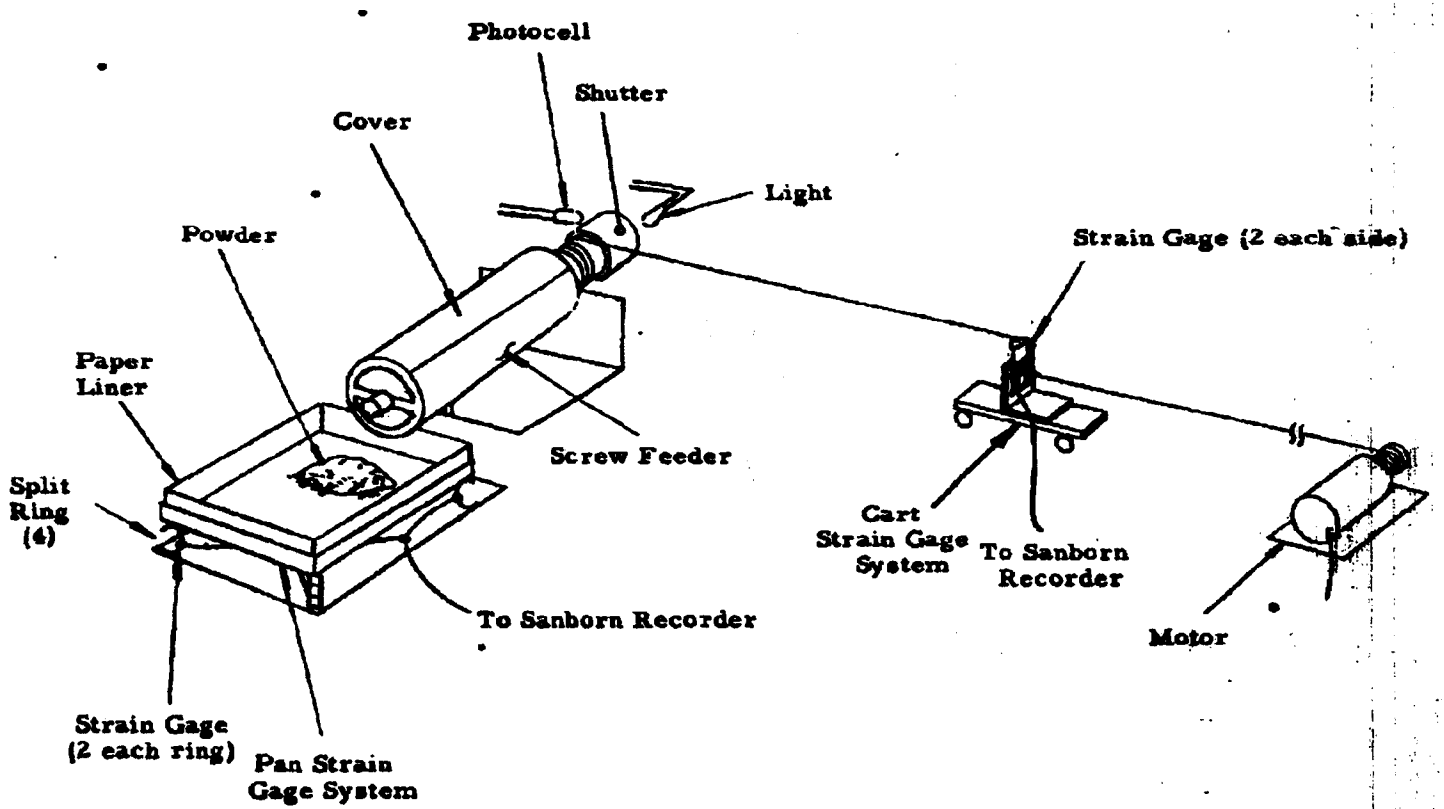

Figure 3.13 Experimental Set-Up for Torque and Output Measurements of Screw Feeder

The torque required to operate the screw feeder was measured with a cantilever beam, strain-gage system. Two strain gages were fastened to each side of a thin aluminum beam. This beam was fastened at one end to a movable cart (Figure 3.13). The cart was pulled along a track by means of a constant speed motor. The torque required to turn the screw was measured and fed to the second channel of the Sanborn recorder.

A photocell-shutter arrangement indicated the completion of each revolution of the screw by a mark on the recorder paper. In this manner, a complete record of torque and powder discharged per revolution was obtained.

3.4.2 Experimental Technique

Preliminary tests were made on the screw feeder with each of the six powders. Routines were established that gave orders of magnitude for torque and efficiency of the feeder. In the case of cornstarch, polyvinyl alcohol and talc, replicate measurements were performed at least 10 times. At least 2 tests were made on the other powders. No attempt was made to compress the powder into the feeder. Each segment of the screw was filled in approximately the same manner yielding nearly constant values for the total amount of powder placed in the feeder in each replicate test. Table 3.3 gives the average bulk density calculated for the powder in the feeder.

At the start of each experiment, the position of the screw was identical. The powder was then placed into the feeder, and the amount of powder determined by weighing. Based on the volume of the feeder (351 cm^3), the average bulk density was calculated. The strain gage weighing system was calibrated with dead weights prior to the test. A cord of sufficient length to permit 12 revolutions of the screw was wrapped around the end of the screw. The resulting lever arm was 1.91 cm. The cord was attached to the cantilever beam on the cart, and the pan strain-gage system was placed

Table 3.3 Torque Required to Move Various Powders through Laboratory Screw Feeder

Powder	Torque (dyne - cm x 10^{-3}) Starting	Maximum	Ratio Maximum Torque / Starting Torque	Initial Charge (gm)	Apparent Bulk Density (gm/cm^3)	Amount Ejected (gm)	Percent Ejected
Cornstarch	600	890	1.48	218	0.621	179	82
PVA 72-51	390	540	1.39	125	0.356	121	97
Talc-18	350	880	2.51	110	0.313	86	78
Sm	860	1940	2.26	135	0.385	98	73
Bg	320	630	1.97	79	0.225	54	68
Saccharin	1120	1900	1.70	98	0.279	60	61

Volume of Screw Feeder: 351 cm^3

under the outlet of the feeder. With both of the strain gage bridges balanced, the continuous speed motor was started which towed the cantilever beam over the track and rotated the screw.

At the first movement of the screw, the photocell circuit noted the movement on the chart. The torque required for this movement was considered to be the starting torque. For each powder tested, the torque continued to increase until approximately one revolution had been completed. This increase was probably due to compaction of the powder. After the first revolution, the torque started to decrease with little more than the inherent friction of the feeder being recorded during the last of the revolutions. Each run required approximately 2.2 minutes for the 12 revolutions required to empty the screw feeder.

3.4.3 Experimental Results

The results of the tests on the screw feeder are presented in two forms. In Table 3.3, the starting and maximum torque, the amount of powder used in the test, the average bulk density of the powder, the amount of powder ejected, and the efficiency of the feeder are recorded. Figures 3.14 and 3.15 present the actual curves from which these data were obtained. The scales noted on the curves in these figures are different for the various powders because of the different attenuator settings required. It should be noted that each powder has its own "signature".

Cornstarch exhibits the most peculiar torque curve in that pronounced stick-slip behavior causes high torque spikes. The amplitude and frequency of the spikes decrease with decreasing amount of powder remaining in the feeder once the maximum value of torque is reached. The maximum torque curve peak is not as defined in the case of cornstarch as with other powders. The small plateau in the amount-ejected curve (fourth revolution) is associated with slip in the motor turning the screw during this particular test. It is not typical of the powder. Cornstarch was ejected in bursts corresponding to the stick-slip torque curve.

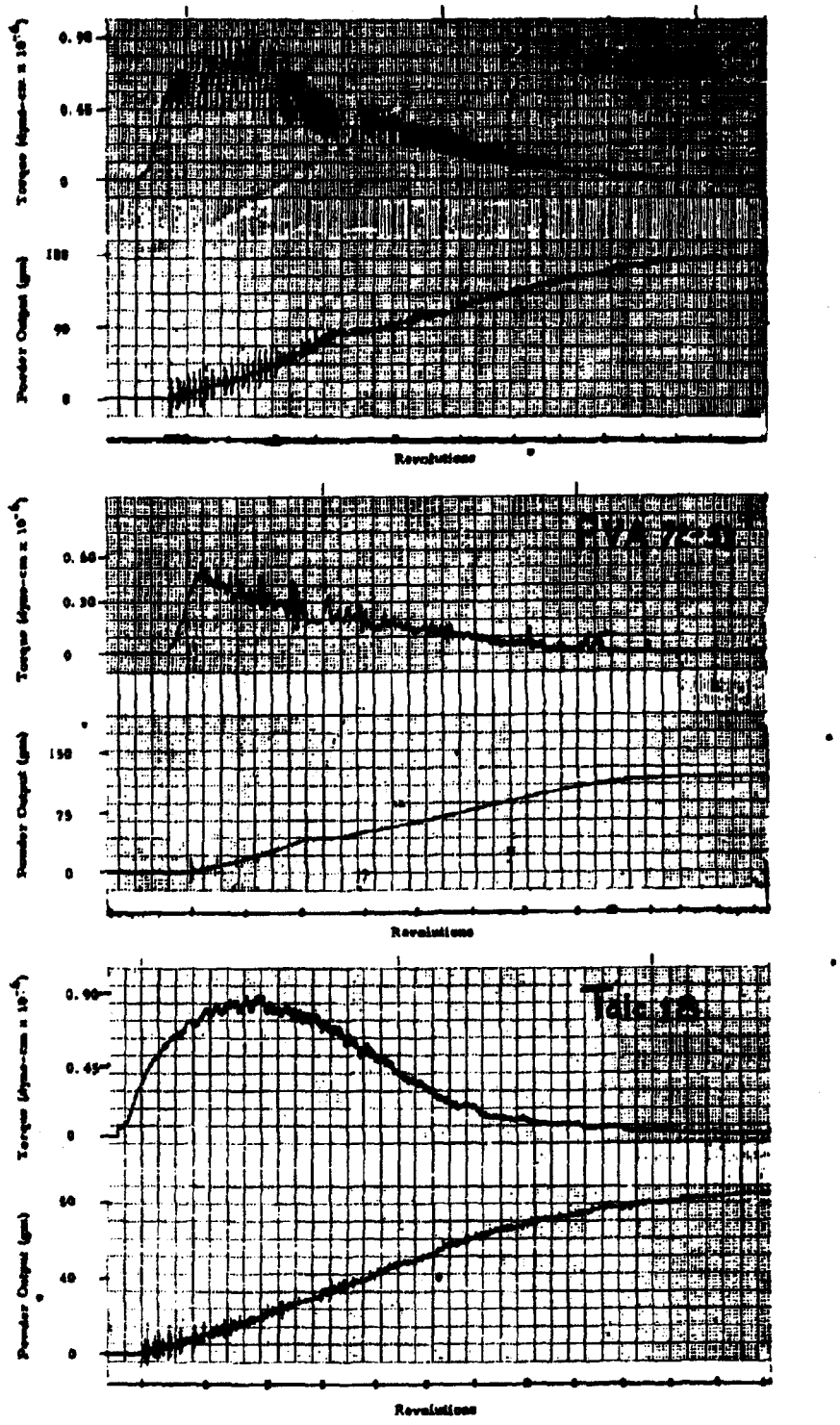

Figure 3.14 Screw Feeder Torque and Output Data for Cornstarch, Polyvinyl Alcohol and Talc Powder

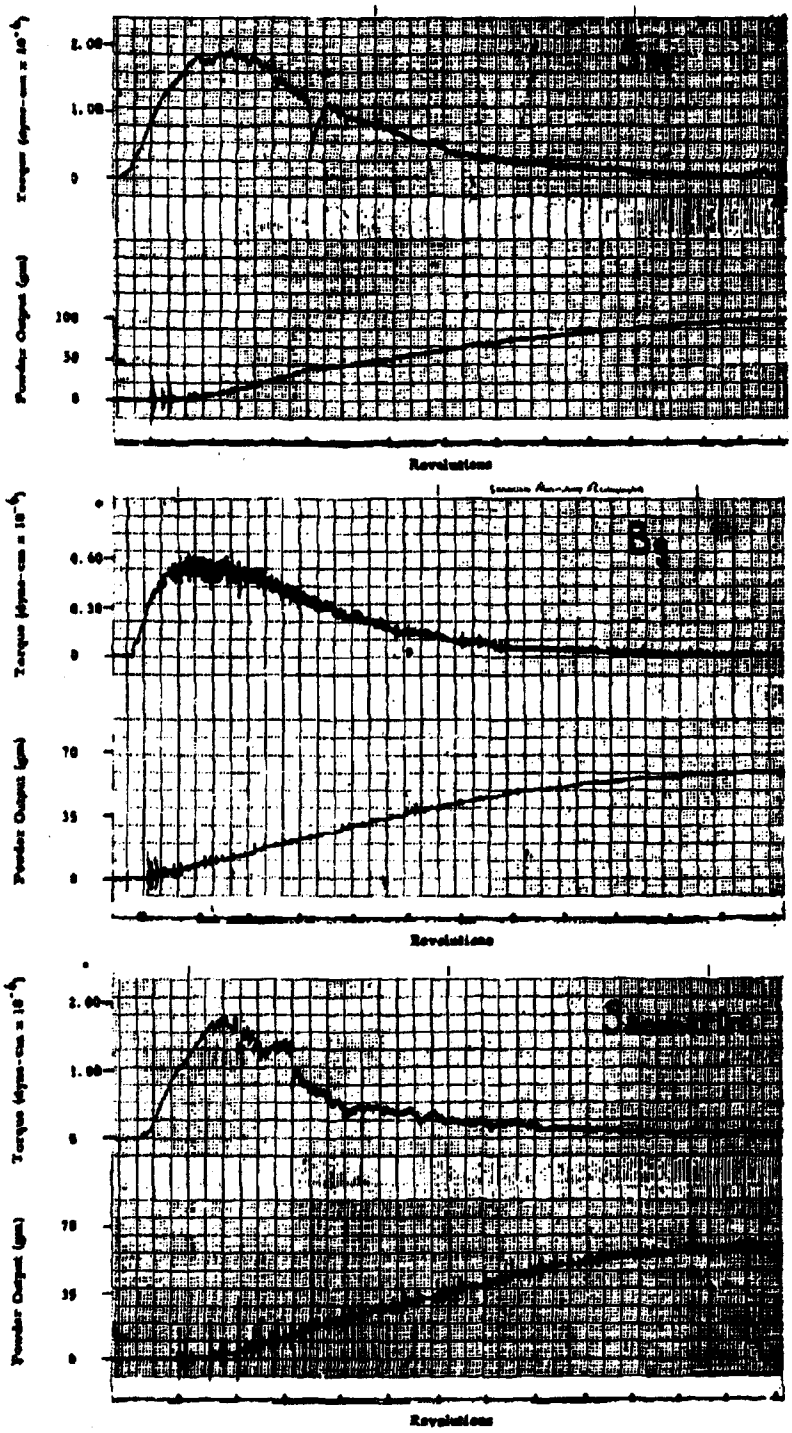

Figure 3.15 Screw Feeder Torque and Output Data for Sm, Bg, and Saccharin Powders

Table 3.3 shows that cornstarch had the highest average bulk density (0.621 gm/cm^3), and the second highest efficiency (82.1%). In the case of each powder except PVA, a core the size of the screw was sheared from the powder leaving a coating on the walls of the feeder approximately 1.5 mm thick. PVA left no such shell and had the highest efficiency (96.8%).

An attempt to relate the "coring effect" of the powders to friction between the powders and the aluminum feeder was made. Because of the extreme difficulty in making a plug of cornstarch for use in the tilting table technique for determining friction coefficients[7], only a rough value of 1.30 to 0.65 for the coefficient of friction against aluminum could be obtained. A similar measurement on PVA yielded a value of 0.26 $\pm$ 0.07. Tests on the other powders yielded values of 0.58 $\pm$ 0.10 for talc, 1.01 $\pm$ 0.40 for saccharin, 0.61 $\pm$ 0.11 for Bg, and 0.65 $\pm$ 0.21 for Sm. A minimum of eight coefficient of friction tests were made on each powder. As expected, the material with the lowest coefficient of friction (PVA) was the one that did not leave a layer of powder on the cylinder.

The powder output curve for PVA is quite smooth, and a nearly uniform rate of emptying is exhibited during the first seven or eight revolutions. The torque curve is highly peaked with the maximum torque being reached early followed by an immediate decrease.

The torque curve for talc is nearly symmetrical for the first five revolutions with the maximum torque occurring after the second revolution. Ejection of the powder occurs at a nearly constant rate for the first seven revolutions and then decreases gradually after that.

Behavior of Sm during ejection is nearly the same as that for talc. The plateau in the output curve after the third revolution is associated with a slip in the screw drive system as is the dip in the torque curve. The shape of the torque curve is similar to that for talc except that the maximum torque occurs earlier. The torque curve during ejection of Sm is much smoother than that for talc with less slipping occurring. The irregular spacing of the revolution markings is due to variation in the screw speed.

As the screw is turned by the cord attached to the strain-gage cart, sticking of the screw may cause it to stop just after a revolution mark. The following slip may turn the screw almost to the point where another revolution mark would be recorded, making the interval slightly longer than it would be if the screw had turned smoothly. In like manner, a shorter than average interval could be formed.

Ejection of Bg from the screw feeder tends to occur in small bursts at times indicated by the small blips on the powder output curve. However, the amount ejected per revolution of the screw is quite uniform for the first seven revolutions. The torque curve indicates stick-slip behavior similar to but not as large in magnitude as that observed with cornstarch. The revolution rate of the screw was unaffected by the stick-slip action. The torque curve for Bg resembles the cornstarch curve in that a small plateau occurs at the maximum value of torque.

With saccharin, ejection of powder in bursts is more evident than with any of the other powders, and this behavior lasts throughout the entire run. The torque curve is more irregular than that obtained for other powders which exhibited little stick-slip action. The required torque appears to level off rapidly, but more torque is required near the end of the run than was found with the other powders tested.

Table 3.3 gives the values of starting and maximum torque, percent ejected, and average bulk density for each test run. Table 3.4 lists the powders in their relative rank according to starting torque, maximum torque, average bulk density, coefficient of friction, and percent ejected from the feeder. The highest value for each parameter has been given the rank of "1". The use of relative rank does not appear to yield any correlation among the various parameters. When data on the shear strength of all the powders are available, further attempts at finding a correlation will be made.

Table 3.4 Relative Ranking of Powders According to Screw Feeder Parameters

Powder	Starting Torque	Maximum Torque	Ratio Maximum Torque Starting Torque	Apparent Bulk Density	Coefficient of Friction versus Aluminum	Percent Ejected
Saccharin	1	2	4	5	2	6
Sm	2	1	2	2	3	4
Cornstarch	3	3	5	1	1	2
PVA 72-51	4	6	6	3	6	1
Talc-18	5	4	1	4	5	3
Bg	6	5	3	6	4	5

General conclusions based on these experiments are: 1) the efficiency of the feeder could be improved by reducing the clearance between the screw and the feeder wall. 2) the particular screw feeder used in this study will eject powder at a fairly uniform rate per revolution only for the first six to seven revolutions; however, at this point approximately half of the amount of powder placed in the feeder has been ejected.

4. EFFECT OF ELEVATED AIRSTREAM TEMPERATURES ON THE VIABILITY OF DRY AEROSOLS OF B. GLOBIGII AND S. MARCESCENS

In a previous report[8] the equipment and methods designed for use in this study were described. Results were presented showing the effect of elevated airstream temperatures upon S. marcescens aerosolized from liquid suspensions.[9]

During the present reporting period, the apparatus and techniques were modified to render the data more reproducible and to adapt the system to the study of aerosols produced from the dry powder. The viability of dry aerosols of B. globigii spores and S. marcescens was studied after exposing them to a series of temperatures ranging from 75°C x 1.12 sec to 130°C x 1.68 sec.

4.1 Modifications in Equipment and Techniques

It was previously reported[8] that the "Y" tube which connected the carboy plenum chamber to the twin 91.5 x 2.5 cm tubes was delivering unequal quantities of aerosol to the two legs of the system. This necessitated the use of a mathematical correction factor when calculating percent recovery. This "Y" tube was redesigned and installed in the system. A series of 22 trials, using both Bg and Sm aerosols, determined that the previous difficulty was overcome. The variation between the two legs of the apparatus is now randomized and is sufficiently small to preclude the use of correction factors.

Because of slight differences in the geometry of the two legs, it was theoretically possible to confound results by residuals of viable spores and cells which might be retained in non-random quantities. A technique was developed whereby the apparatus could be easily disassembled at the completion of an experiment, washed, chemically disinfected, dried, and reassembled in a short period of time.

Whereas dry aerosols of Bg spores could be generated in the plenum chamber by previously described techniques to yield satisfactory and reproducible results, some difficulty was experienced during attempts to aerosolize dry powders of Sm with the vaponephrin nebulizer. It was therefore necessary to develop a new method which would produce relatively stable aerosols of dry Sm powders. The following method was found to be satisfactory:

A 10 mm diameter Dental Dam diaphragm was fitted into a 4-inch length of 1/4-inch O.D. copper tubing. Approximately 0.30 gm Sm which had been stored in a dry box for 14 hours was loaded into the pipe. The open end of the pipe was fitted tightly onto a dry nitrogen pressure tank, and the powder was exploded into the carboy under 74 psi gauge pressure. The powder was not allowed to settle but was drawn immediately via the "Y" tube into the twin legs of the apparatus, and sampling was continued for 10 minutes in All Glass impingers. The procedures of diluting and plating were performed according to protocols previously described.

4.2 Reproducibility of Results

The data reported in Table 4.1 show the reproducibility obtained upon splitting dry aerosols of Bg and Sm in the two legs of the elevated airstream temperature apparatus. In all of these trials, the organisms were aerosolized into the carboy plenum, passed through the twin legs of the apparatus and sampled in liquid impingers by methods described in previous reports. Since these trials were designed to measure reproducibility, no heat was applied in the insulated tube. Each replicate represents the average results of six plates.

Table 4.1 Reproducibility of Flow-Splitting Device in Elevated Airstream Temperature Apparatus

Date	Culture	Replicate	Leg A	Leg B	Replicate Mean
10/9/61	Bg	1	85×10^6	72×10^6	$78.5 \pm 6.5 \times 10^6$
		2	63×10^6	68×10^6	65.5 ± 2.5
10/10/61	Bg	1	101×10^6	100×10^6	100.5 ± 0.5
		2	81×10^6	80×10^6	80.5 ± 0.5
10/11/61	Bg	1	87×10^6	85×10^6	86.0 ± 1.0
		2	98×10^6	83×10^6	90.5 ± 7.5
10/23/61	Bg	1	54×10^6	41×10^6	47.5 ± 6.5
		2	58×10^6	47×10^6	52.5 ± 5.5
10/24/61	Bg	1	56×10^6	51×10^6	53.5 ± 2.5
		2	87×10^6	100×10^6	93.5 ± 6.5
		3	86×10^6	113×10^6	99.5 ± 13.5
10/26/61	Bg	1	31×10^6	28×10^6	29.5 ± 1.5
		2	30×10^6	20×10^6	25.0 ± 5.0
		3	24×10^6	24×10^6	$24.0 \pm < 1$
10/31/61	Bg	1	65×10^6	82×10^6	73.5 ± 8.5
		2	69×10^6	88×10^6	78.5 ± 9.5
11/2/61	Bg	1	50×10^6	36×10^6	43.0 ± 7.0
		2	53×10^6	47×10^6	90.0 ± 3.0
		3	70×10^6	52×10^6	61.0 ± 9.0
11/15/61	Sm	1	125×10^6	148×10^6	136.5 ± 11.5
		2	111×10^6	84×10^6	97.5 ± 13.5
		3	125×10^6	124×10^6	124.5 ± 0.5
All Trials:			69.5×10^6	71.5×10^6	$70.5 \pm 1.0 \times 10^6$

4.3 Viability of Dry Aerosols of Bg and Sm

Initial conditions used for investigating the effect of temperature and time of exposure on aerosols of dry Bacillus globigii spores were 125°C and 1.68 seconds. The data obtained are summarized in Table 4.2 and are plotted in Figure 4.1. The data indicate that these conditions have no measurable influence on the viability of the Bg spores. In view of these results, no experiments were performed at lower temperatures or shorter exposure times.

In contrast, there was a pronounced viability loss with Serratia marcescens upon heating to temperatures between 75°C and 130°C for periods of 1.12 to 1.68 seconds. These data are summarized in Table 4.3 and are plotted in Figure 4.1. The original viability of the powder used in the aerosols was 8.0×10^{10}/gm. These results confirm the conclusion which was reached upon the basis of experiments performed with aerosols of Sm generated from liquid suspension; namely, that the viability of Sm is substantially reduced upon exposure to elevated temperature airstreams for very short periods of time.[9]

These experiments with Bg and Sm clearly illustrate that the potential effect of hot gases from jet engine exhausts on the viability of BW aerosols will depend largely on the sensitivity of the particular organism being disseminated. Future experiments will investigate the effect of shorter exposure times on viability loss in dry Sm aerosols, and the effect of higher temperature on Bg aerosols. Temperatures somewhat higher than 125°C are of interest in certain cases. A recent analysis of jet plume mixing[9] concluded that for the case of a small drone, where the disseminator mounting station is approximately three feet from the center line of the engine, the aerosol entering the plume would be exposed to temperatures up to 420°F (216°C) under certain assumed conditions of operation.

Table 4.2 Viability of Dry Aerosols of Bg at 125°C for 1.68 Seconds
(Bg from Lot No. X-12 Aerosolized with DeVilbiss Generator)

Replicate	Heated	Control	Average % Recovery
1	29×10^6	22.5×10^6	
2	15×10^6	11×10^6	
3	12.5×10^6	21×10^6	102%
4	13×10^6	13×10^6	

Table 4.3 Viability of Dry Aerosols of Sm at Various Exposures
(Sm from Pool #7 Aerosolized by Explosion)

Temperature	Time	Heated	Control	Average % Recovery
75°C	1.12 sec	161×10^6	230×10^6	
		86×10^6	119×10^6	71.0%
		130×10^6	182×10^6	
	1.68 sec	37×10^6	79×10^6	
		39×10^6	63×10^6	55.0%
		51.5×10^6	91×10^6	
100°C	1.12 sec	77×10^6	177×10^6	
		68×10^6	113×10^6	48.3%
		94×10^6	202×10^6	
	1.68 sec	76×10^6	181×10^6	
		54×10^6	127×10^6	44.0%
		61×10^6	127×10^6	
125°C	1.12 sec	55×10^6	175×10^6	
		80×10^6	261×10^6	34.0%
		117×10^6	302×10^6	
130°C	1.68 sec	8×10^6	175×10^6	
		4.5×10^6	141.5×10^6	3.9%
		5×10^6	149×10^6	

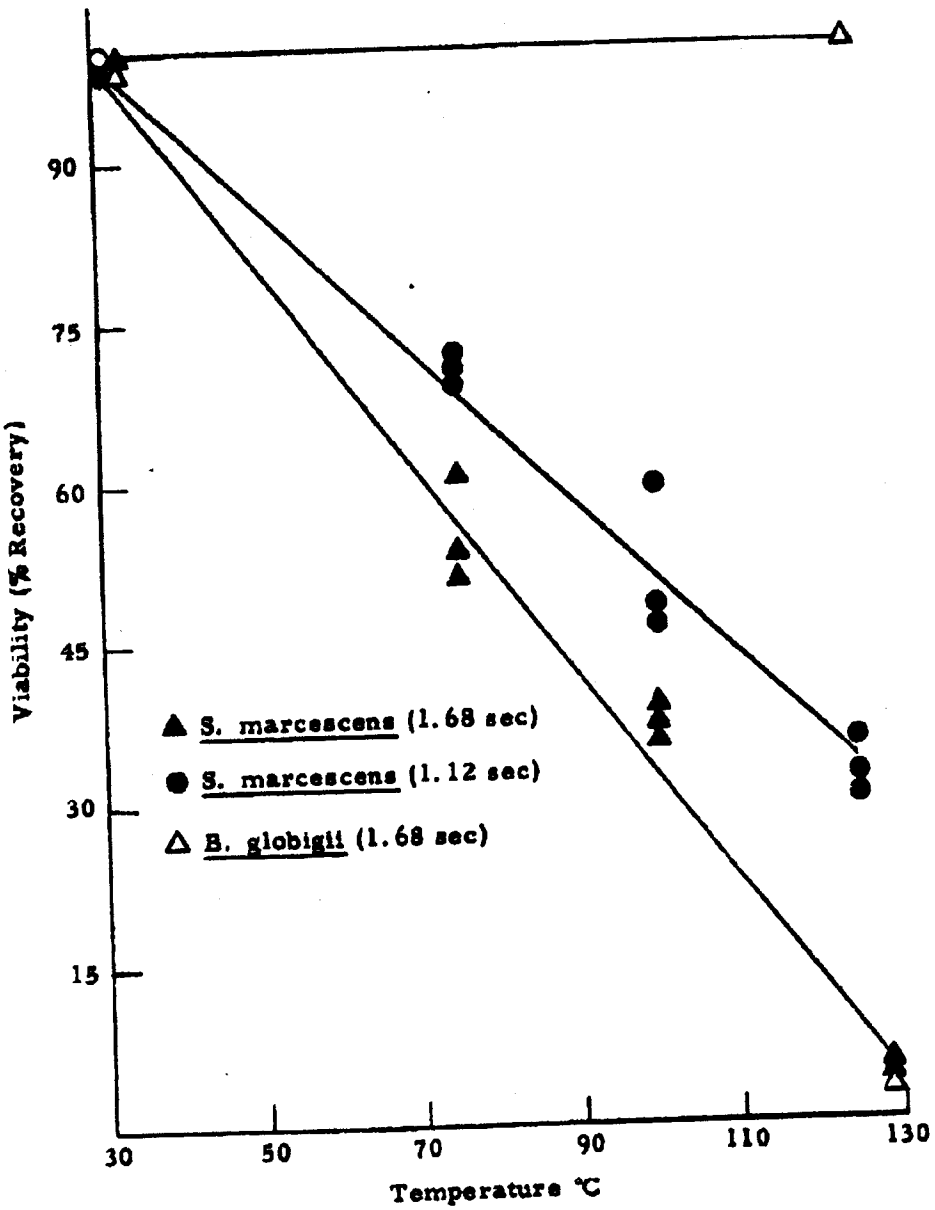

Figure 4.1 Viability of Dry Aerosols of B. globigii Spores and S. marcescens in Elevated Air Temperatures

4.4 Effect of Compaction on the Viability of S. marcescens

A previous report[10] described the equipment and techniques used to measure the effect of compaction on the viability of dry Sm powders. Essentially the method involved determination of viable count of Sm pellets (density: 0.48 gm to 0.77 gm) which had been prepared under different compaction pressures and comparison of viable count of the uncompressed powder from which the pellets had been manufactured. The results of some of these trials are summarized in Table 4.4. The results suggest that there might be a slight effect of compaction on apparent viability since the highest pressures studied yielded the lowest recoveries. However, it is possible that the compression process introduces artifacts in a viability study. On the one hand, compaction pressures generate shearing forces which can deagglomerate clumps and perhaps even fracture individual particles yielding higher apparent recoveries from the compressed sample. On the other hand, a pellet produced by compaction is exceptionally difficult to disperse by mechanical shaking in a diluent, and would yield apparently lower recoveries from the compressed sample unless dispersion is complete. Superimposed on these phenomena, is the possibility that compression might alter the true viability of the cell.

In order to overcome some of the confounding variables, and to study the effect of compression on true viability, several different experiments were performed with the 30-pound compression weight. In one set of experiments, the compacted pellets were disintegrated by mechanical shaking, resulting in apparent recoveries of 69.5 to 72.5 percent. In the second set of experiments, both the control powder and compacted pellet were disintegrated into the diluting solution by means of a tissue homogenger. These results showed that the viability of the compacted samples ranged from 86 to 96 percent of the original powder. On the basis of the latter results, it would be concluded that compaction is not deleterious to viability.

Obviously, further work remains to be done on developing technically precise methods of distinguishing between loss of true viability and apparent change in count due to mechanical artifacts. Once this is accomplished, the effect of rate of compression on viability will be investigated.

Table 4.4 Effect of Compression on Viability of Sm Powder (Sm from Pool #7)

Compression Weight	Density of Pellet	Viable Count (Control)	Percent Viability
*500 gm	0.5037	78.5×10^6/gm	82.0%
	0.5225		76.5%
	0.5568	70.0×10^6/gm	77.0%
	0.5411		86.0%
	0.5445		76.0%
*1500 gm	0.5318	65.0×10^6/gm	96.0%
	0.5947		90.0%
	0.5755		86.0%
*13.62×10^3 gm	0.7414	73×10^6/gm	72.5%
	0.7516		69.5%
	0.7982	66×10^6/gm	71.5%
	0.7585		69.5%
**13.62×10^3 gm	0.772	67×10^7/gm	96%
	0.762		93%
	0.692		86%

* Pellet and control disintegrated into diluent by mechanical shaking.
** Pellet and control disintegrated into diluent with tissue homogenger.

[redacted]

5. DISSEMINATION AND DEAGGLOMERATION STUDIES

5.1 Introduction

Studies were continued during this reporting period to determine the description of the wind tunnel aerosol, generated by a new, combined mechanical-pneumatic disseminator which was built to simulate a design concept being considered for the prototype disseminator.

Both compacted and uncompacted Sm were tested in the disseminator at bulk densities ranging from 0.33 to 0.65 gm/cc. The Sm moisture content was maintained at approximately 1.7 percent by storing and working with the material in a dry box prior to the test runs.

Analysis of the aerosol was made by two methods. First, fine agglomerates were studied by sampling them on Millipore filters with a secondary sampling system which collected one percent of the material drawn into the high velocity sampling probe. In microscopic analysis of the collected material, the amount of agglomerates in the 1 to 5 microns, 5 to 20 microns, and greater than 20 microns ranges were counted. The majority of agglomerates in this category consisted of doublets and triplets. To further determine the reduction in deagglomeration efficiency, the results were analyzed on the basis of the mass of effective 1 to 5-micron particles which are combined to form agglomerates greater than 5 microns. In this work the agglomerates greater than 5 microns were studied in detail as to their composition and size.

While running tests with the filter system, it was observed that there was present in the aerosol a relatively small number of larger agglomerates up to about 500 microns in size. However, due to their low concentration it was not feasible to study them with the filter sampling technique, where only a small percentage of the aerosol is collected. Therefore, an impactor system was designed and fabricated which collected essentially

[redacted]

all of the agglomerates greater than 20 microns in the tunnel. The analysis consisted of mass measurements, microscopic observations, and Whitby centrifuge analysis.

Two runs were made with the pneumatic system where high speed motion pictures were taken to enhance an understanding of the aerosol aerodynamic breakup process.

5.2 Pneumatic Disseminator

All the wind tunnel tests and studies during this reporting period were conducted with a mechanical-pneumatic disseminator which simulates the injection region of a particular prototype design, discussed in Section 6. The system, shown in Figure 5.1, uses the same piston-type disseminator that has been employed in all previous tests. However, in this case Sm is injected into a small chamber which is maintained at an air pressure of 5 psig. The air then is utilized to transport the material into the wind tunnel airstream.

In operating this type of system it is desirable from the standpoint of air or gas consumption to maintain a highly concentrated bed of powder above the discharged orifice. In this manner the air flow rate is minimized at the orifice. Thus, there is no intention of aerosolizing the material before it reaches the wind tunnel – breakup should occur in the tunnel under aerodynamic forces of the airstream.

It is apparent that in the case of compacted materials there is some breakup in the air chamber due to mechanical forces present when part of the material is impacted on the chamber wall. These forces do not completely break down the slugs into basic particles. We believe that the physical condition of the material is similar to that which will be produced in the actual prototype due to mechanical forces associated with the shearing process and mechanical mixing.

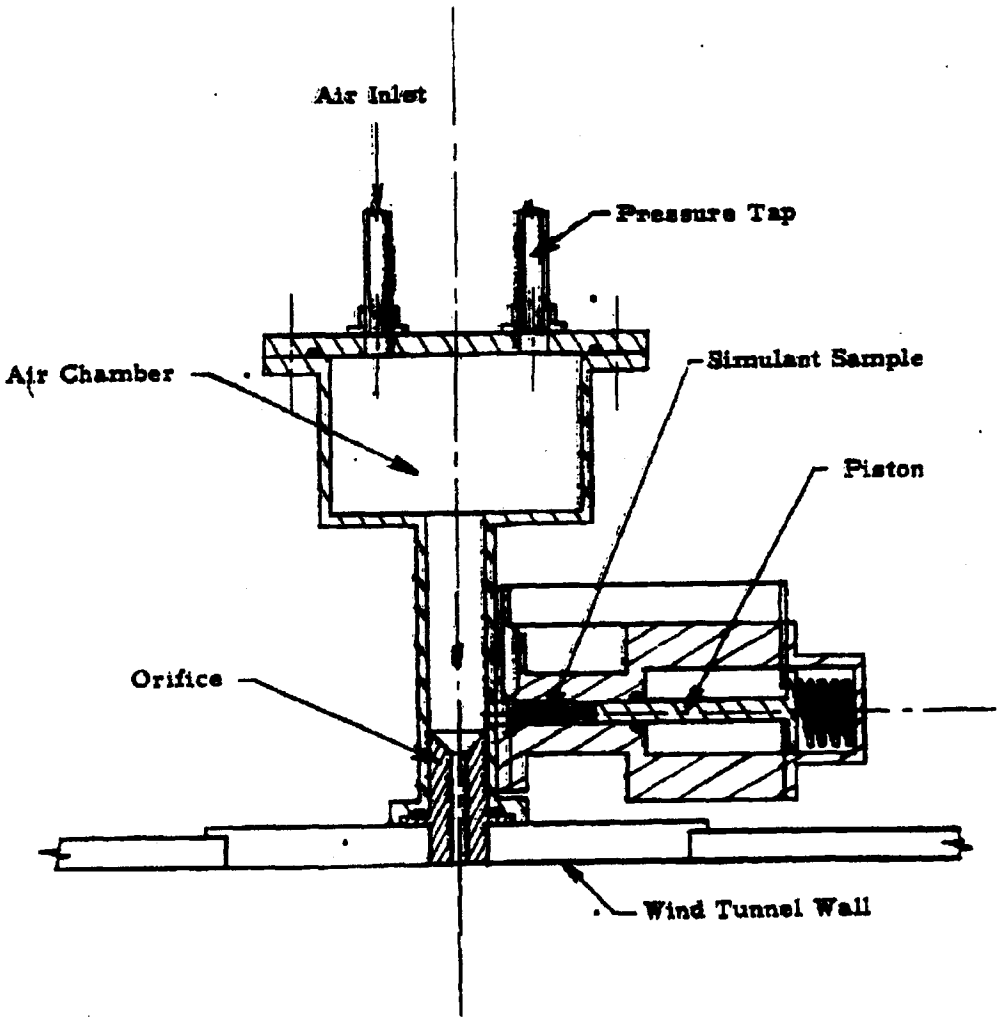

Figure 5.1 Mechanical-Pneumatic Disseminator Model

As a result of earlier tests of this injection technique, it was found that to obtain an instantaneous bed in the air chamber, it was necessary to inject the material just upstream of the orifice. Thus, the orifice was made longer than anticipated in a prototype.

For wind tunnel operation the air pressure is regulated to 5 psig before the run; i. e., air flows through the chamber before Sm is introduced into it. Since this is somewhat different from the case of continuous operation in the prototype, it was desirable to look closely at the flow of material as it enters the wind tunnel. Thus, high speed photography was employed again using the same technique and equipment as was previously used.[11]

The pictures show that there is a short period of high powder flow rate which begins soon after the mechanical injector starts filling the air chamber. However, as the chamber empties, some material sticks to the walls and breaks off in chunks causing very short bursts of high aerosol concentration and a gradual trailing off of the process in the form of a light aerosol cloud.

It appears very likely that during 0. 01 seconds of the runs a fairly dense bed exists in the air chamber. Injection velocities taken from the pictures indicate that the average flow rate is about 2. 0 pounds per minute during this period.

Other interesting factors are also brought out by the pictures. For example, even though the injection velocity is from two to four times that of the previous studies, the bulk of material does not penetrate any further into the wind tunnel. The reason is that the material is dispersed quicker and accelerated faster down the wind tunnel.

One difference exists as a result of increased injection velocity. The larger agglomerates, approximately 300 microns in size, are separated from the dense cloud of dispersed Sm due to their high inertia. Some of these can be seen to penetrate into the airstream without undergoing

aerodynamic breakup. These will be discussed later in terms of their concentration. Comparisons of photographs at conditions of 0.33 and 0.60 gm/cc bulk density showed that a substantially larger number of agglomerates in the 100 to 300-micron range exist in the Sm entering the tunnel for the latter case. However, a large majority of these undergo aerodynamic breakup by surface shear stresses during acceleration. So the net difference between the two conditions appears to be small from the standpoint of these large scale agglomerates.

Another interesting observation that has been made is that the aerosol cloud tends to spread in the tunnel by turbulent diffusion which is in part produced by the injection jet.

5.3 Sm Dissemination – Small Scale Agglomerate Study

In sampling the wind tunnel aerosol it has been found that agglomerates ranging from 1 to 500 microns are present in decreasing numbers with increasing size. The small scale agglomerates in the 1 to 20-micron range can best be analyzed by using filtration and microscopic methods, while those larger than this are in such low concentration that it is not practical to analyse them in this way. Thus, an impaction technique discussed in the following section was employed for agglomerates greater than 29 microns.

A secondary filter sampling system was constructed for the work on small agglomerates to enable us to disseminate approximately 1 cc of Sm into the tunnel and yet reduce the particle concentration on the filters to a low enough value that microscopic methods could be used. Figure 5.2 shows the new filtering arrangement. The secondary system samples from the large section of the high velocity sampling probe where the velocity is on the order of 10 feet per second. A standard 47 millimeter membrane filter holder is employed with Type AA Millipore filters which have a pore size of 0.8 micron. Thus, the secondary filter collects about one percent of the aerosol which enters the high velocity sampling probe.

The unit was tested for its isokinetic characteristics by comparing on a number basis the particle size distribution of the collected sample with the controlled distribution as shown in the previous report[12]. The agreement between these cases was very good, indicating satisfactory operation of the new system.

All tests conducted in this part of the study were carried out at wind tunnel Mach number 0.5. The high velocity sampling probe was located at the point of high aerosol concentration, namely 0.63 centimeters from the top wall. The major parameter investigated was Sm bulk density, which varied from 0.33 to 0.65 gm/cc. The material had a moisture content of about 1.7 percent.

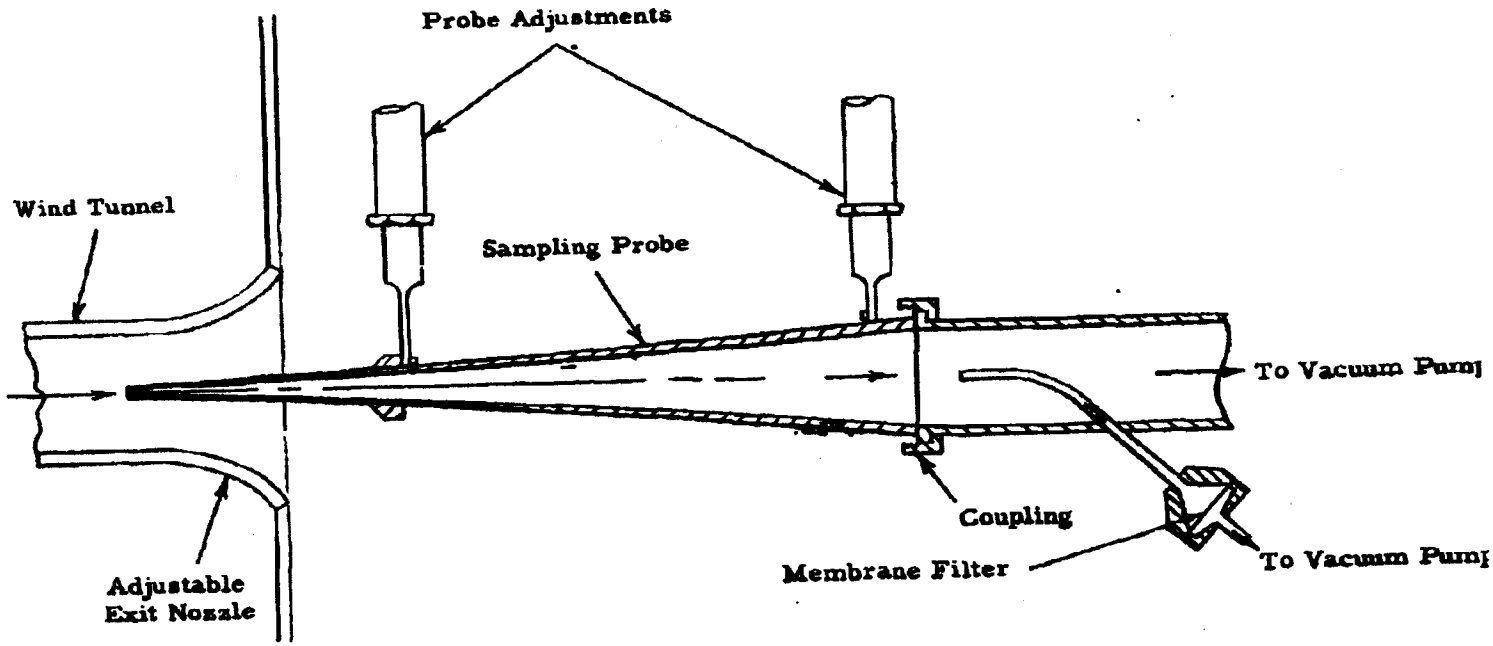

Figure 5.2 High Velocity Sampling Probe and Secondary Filtration System

In analysing the filters a light microscope was used at X600 for sufficient resolution to count particles down to about 0.7 micron. The first step was to count a combined total of at least 1000 basic particles and agglomerates for each test. The latter were classified into three size ranges: 1 to 5 microns, 5 to 20 microns, and greater than 20 microns. This breakdown was made because those in the 1 to 5-micron range do not reduce the effectiveness of the aerosol as do all the others.

Microscopic observations of a large number of particles and agglomerates on the filters indicate that these small-scale agglomerates were primarily composed of doublets and triplets. In the analysis, all particles that appeared to have any contact whatsoever were considered as agglomerates. It is obvious that some of these are formed as a result of filtration, one particle falling upon the other. The number of doublets formed due to this probability is now being considered; however, in this discussion we will omit this factor and discuss only the upper limiting condition.

A photomicrograph of a typical field on the filter is shown in Figure 5.3. Note that to a very large extent the material appears as basic particles - doublets and triplets are quite rare.

Results of seven tests are shown in Table 5.1 where the number of agglomerates in the three size ranges are compared with the total concentration of particulate material on the filters. It can be seen that the largest percentage of small-scale agglomerates is in the 1 to 5-micron size range. Above 20 microns there were no agglomerates observed in any run when 1000 particles or more were counted. Figure 5.4 shows the data plotted over the Sm bulk density range 0.33 to 0.66 gm/cc.

Important conclusions of this work are that the amount of agglomerates present in the aerosol increases only a small amount with bulk density. Also, the number of agglomerates in the 5 to 20-micron range are relatively small on the number basis.

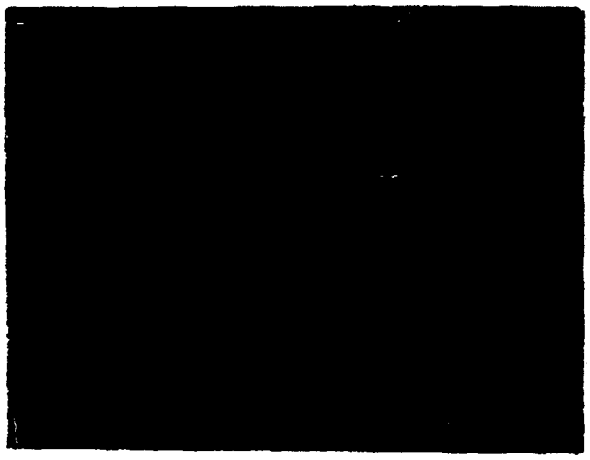

ρ_B = 0.33 (X-300)

Figure 5.3 *Photomicrograph of Filter Samples of Sm Aerosol*

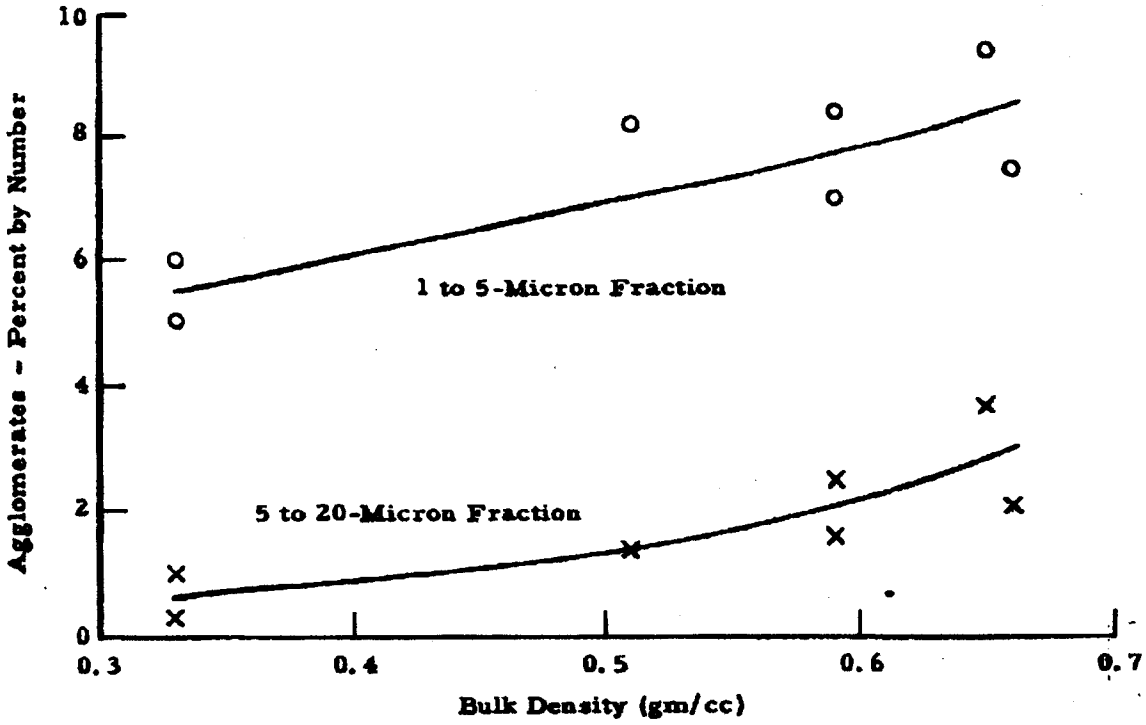

Figure 5.4 Percentage of Sm Aerosol Particles (by number) Consisting of Agglomerates in the 1 to 5-Micron and 5 to 20-Micron Ranges (Wind tunnel Mach number 0.5; sampling position – 0.63 cm below tunnel top wall)

Table 5.1 Small-Scale Agglomeration of Sm Simulant Disseminated in Mach Number 0.5 Airstream with Pneumatic System

Sm Bulk Density	Filter Particle Concentration	Percent of Particulate Material as Agglomerates 1 to 5μ	5 to 20μ	>20μ
0.33 gm/cc	49.5×10^4	5.0	0.3	Negligible
[illegible]	[illegible]	6.0	1.0	Negligible
0.51 gm/cc	37.3×10^4	5.6	1.4	Negligible
0.59 gm/cc	46.2×10^4	7.0	2.5	Negligible
0.59 gm/cc	31.1×10^4	8.4	1.6	Negligible
0.65 gm/cc	36.5×10^4	9.4	3.7	Negligible
0.66 gm/cc	36.5×10^4	7.5	2.1	Negligible

To determine the effect that small-scale agglomeration has on the effectiveness of the disseminator the analysis must be placed on a mass basis. Therefore, we have made calculations on the amount of mass in the 5 to 20-micron agglomerates which consists of individual particles in the 1 to 5-micron range. To carry out these calculations it was necessary to determine the characteristics of the larger agglomerates. Thus, 100 of them were observed in detail and the individual particles contained therein were sized. Table 5.2 provides a description of the agglomerates with a tabulation of the basic particles in the 1 to 5-micron size range.

In general, basic Sm particles are known to have a platelet shape. However, in the 1 to 5-micron size range they can be assumed to approach a spherical shape for these calculations.

The mass of material in the 1 to 5-micron range in the original sample was also determined. It was based on the particle size distribution by number for the material as determined under a light microscope. The distribution, shown in Figure 5.5, indicates that about 79 percent of these particles by number are in the 1 to 5-micron range, while only 5 percent are greater than 5 microns.

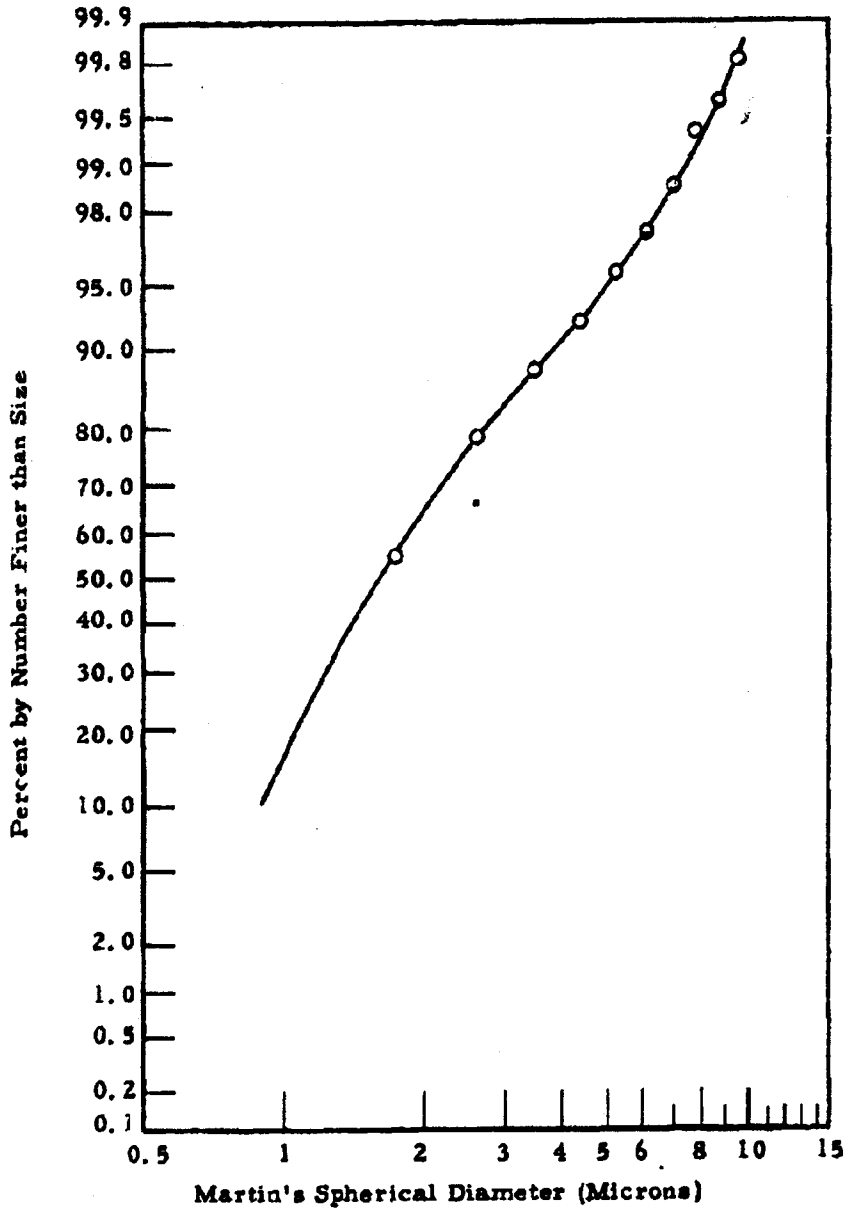

Figure 5.5 Particle Size Distribution of Sm Aerosol on a Number Basis

Table 5.2 Description of Agglomerates in the 5 to 20-Micron Range

Number of Particles in Agglomerates	Total Number of Agglomerates	Number of 1 to 5-Micron Particles Comprising Agglomerates			
		1 to 2μ	2 to 3μ	3 to 4μ	4 to 5μ
2	72	1	3	13	26
3	16	2	4	5	7
4	8	4	3	2	5
5	2	1	1	1	2
6	1	1	1	-	2
8	1	1	2	2	1
	100	10	14	23	43

To determine the loss of effectiveness of the dissemination process, let us use as an example the data at bulk density 0.6 shown in Figure 5.4. For each group of 100 particles present in the aerosol (basic and agglomerated) there are 79 basic and agglomerated particles in the 1 to 5-micron range and 2.2 agglomerates in the 5 to 20-micron range.

Based on data in Table 5.2 the mass of useful material in an average 5 to 20-micron agglomerate is 37.4×10^{-12} gm. The 79 particles in the lower range have a total mass of 853×10^{-12} gm. Thus, the loss in effectiveness of 1 to 5-micron material in the dissemination process due to small-scale agglomeration in this case is:

$$\frac{\text{ineffective mass}}{\text{effective mass} + \text{ineffective mass}} =$$

$$\frac{2.2 \times 37.4 \times 10^{-12}}{853 \times 10^{-12} + 2.2 \times 37.4 \times 10^{-12}} = 8.8\%$$

Figure 5.6 gives the results of these calculations over the bulk density range 0.33 to 0.66 gm/cc. It should be remembered that these figures represent the upper limits on a loss of effectiveness. The factor of doublet formation due to filtration tends to make this value greater than in the actual aerosol.

5.4 Sm Dissemination – Large Scale Agglomerate Study

It was stated earlier that a relatively small number of large agglomerates on the order of 100 to 500 microns were found in the study discussed in Section 5.1. Due to their small number, however, they could not be studied from the statistical standpoint. Consequently, an impactor was designed which could sample the full discharge of the tunnel and collect sufficient material for analysis. Based on the impaction efficiency data of Rans[13], it was found that by mounting the impactor a short distance downstream of the tunnel exit a 50 percent cutoff could be obtained at about the 6-micron size. This holds true for the wind tunnel Mach number condition 0.5. Thus, the collection efficiency for all agglomerates above 20 microns would be near 100 percent.

The analysis technique employed was to weigh the material on the impactor plate and determine the amount sampled which consisted of large-scale agglomerates. This quantity was then compared with the amount disseminated to obtain the percentage of the aerosol which is composed of these agglomerates.

The impactor is shown in Figure 5.7. The face of the unit consists of two microscopic slides mounted end to end in the vertical plane. Surrounding these is an aluminum plate with an outside dimension of seven inches by seven inches. The combined collector plate can be weighed in an analytical balance for fine accuracy. The glass slides make possible microscopic analysis of a representative portion of the collected material.

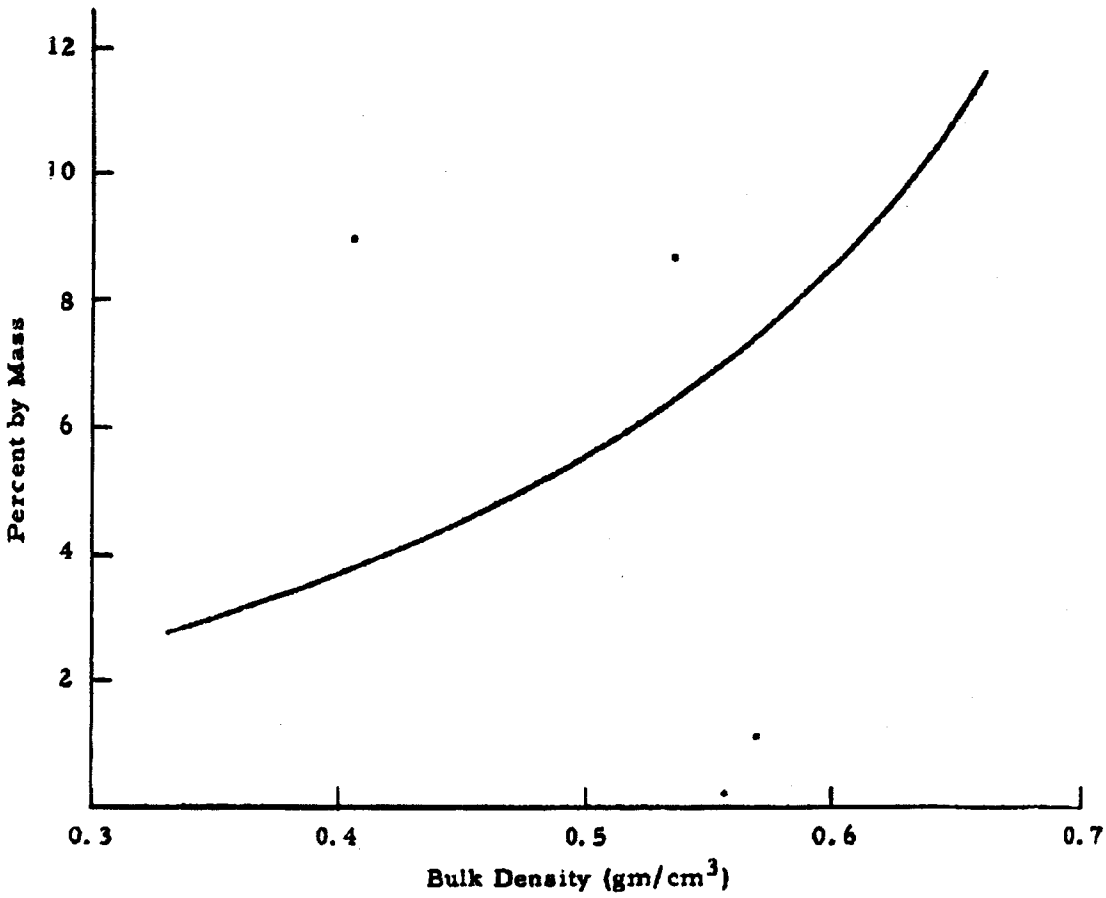

Figure 5.6 Loss in Effectiveness of 1 to 5 Micron Sm Particles Due to Small Scale Agglomeration

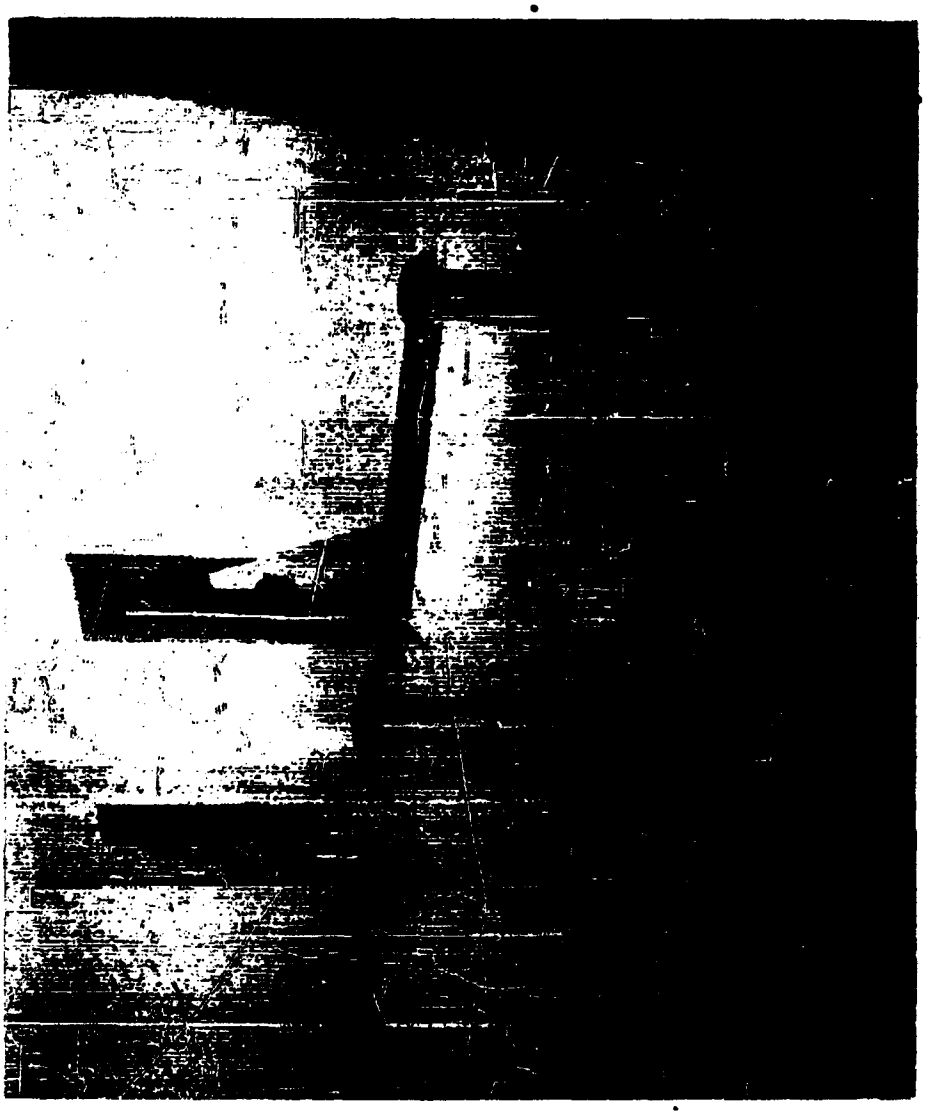

Figure 5.7 Wind Tunnel Full-s[illegible] mpa[illegible]

The general collection pattern on the plates revealed that the large agglomerates were mainly concentrated in the bottom half of the tunnel while the larger basic particles were found in high concentration on the top half of the tunnel. As an example, Figure 5.8 shows photomicrographs of the top and bottom sections on the impactor. Note the large 120-micron agglomerate - many of its individual particles can be observed.

The amount of material greater than 20 microns was estimated by using the Whitby centrifuge. Other methods such as counting and calculating were found less accurate. A method of weighing the slides separately and then estimating the relative mass in the large agglomerates agreed quite well with the results. It is believed that these large agglomerates are quite strong in most cases since they withstand the dissemination process without breaking up. Since the amount of mass in agglomerates must be small, it appears that any breakup in the centrifuge has a minor effect on the over-all results.

Figure 5.9 shows both the percentage of disseminated material collected and the percentage of the original material which is in the greater than 20-micron range. The presence of agglomerates is essentially independent of the bulk density. They represent about 2 percent of the total mass disseminated in all cases which is considered to be quite small.

The deagglomeration studies during this period have shown that compacted Sm with bulk densities as high as 0.65 gm/cc can be disseminated with the mechanical-pneumatic system almost as effectively as the uncompacted material. The results indicate that the maximum loss in effectiveness of the disseminator due to agglomeration of particles in the 1 to 5-micron range is about 12 percent by mass. It is anticipated that this figure will be reduced by future considerations as to the origin of the doublet and triplet agglomerates observed on the filter samples. Since this work has only been conducted at tunnel Mach number 0.5 a portion of it will be reproduced at Mach number 0.8 in the next reporting period.

Top Slide (X-300)

Bottom Slide (X-300)

Figure 5.8 Photomicrographs of Impactor Sample (Sm)

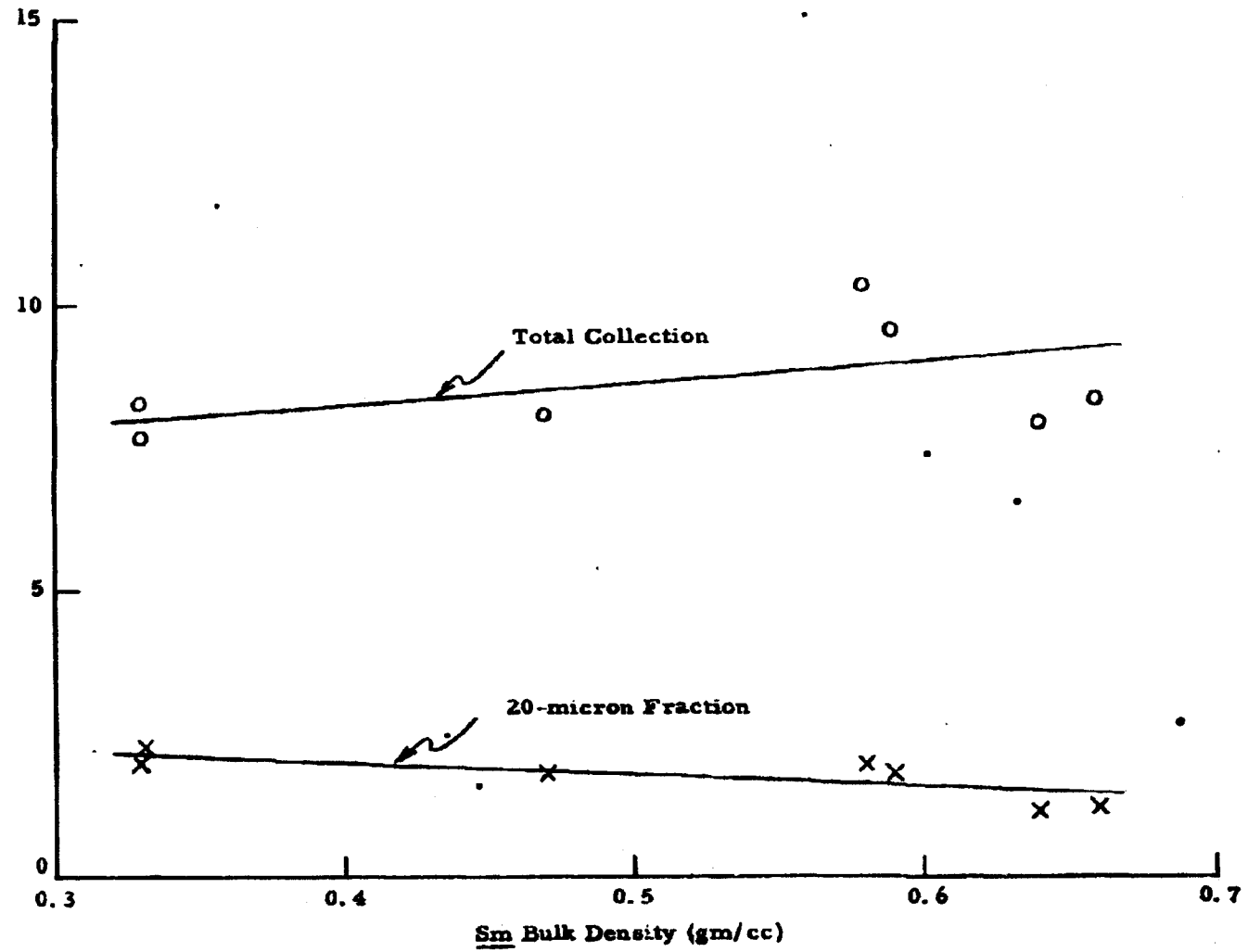

Figure 5.9 Mass of Sm Collected on Impactor as Compared to Amount Disseminated (Wind Tunnel Mach Number 0.5)

6. EXPERIMENTAL DRY-AGENT DISSEMINATOR

A design concept for a dry-agent disseminator was presented in the fifth quarterly progress report[14]. A program has been initiated in which a full size disseminator based on this concept is to be tested in the laboratory to demonstrate the feasibility of such a disseminator and to obtain necessary engineering design data. An experimental disseminator and some of the associated equipment required for the test program were designed and fabricated. The experimental unit and some of the test plans are discussed in the following programs.

6.1 Description of Experimental Dry-Agent Disseminator

The experimental dry-agent disseminator for laboratory studies is shown in Figure 6.1. This unit incorporates the principal features of the airborne unit described in Reference 14, except that no attempt was made to use lightweight structural components in this first unit.

Dry-agent simulant material is to be compacted in the cylinders on both sides of the center section. The materials will be forced into the center section by pistons mounted at the ends of the unit. The pistons are moved toward the center by long screws, one left-handed and one right-handed, driven from one end of the disseminator. The screws are connected at the center through the hub of the disaggregator which rotates with the screws. As the disaggregator rotates it shaves off powder which falls into the center section where it mixes with gas and flows through the discharge orifice in the bottom of the center section.

The dimensions selected for the experimental unit are not necessarily those which will be used in the airborne developmental model, but the length and diameter of the cylinder are large enough so that the experimental unit is actually a full-scale model. Some of the more important geometric data are presented as follows:

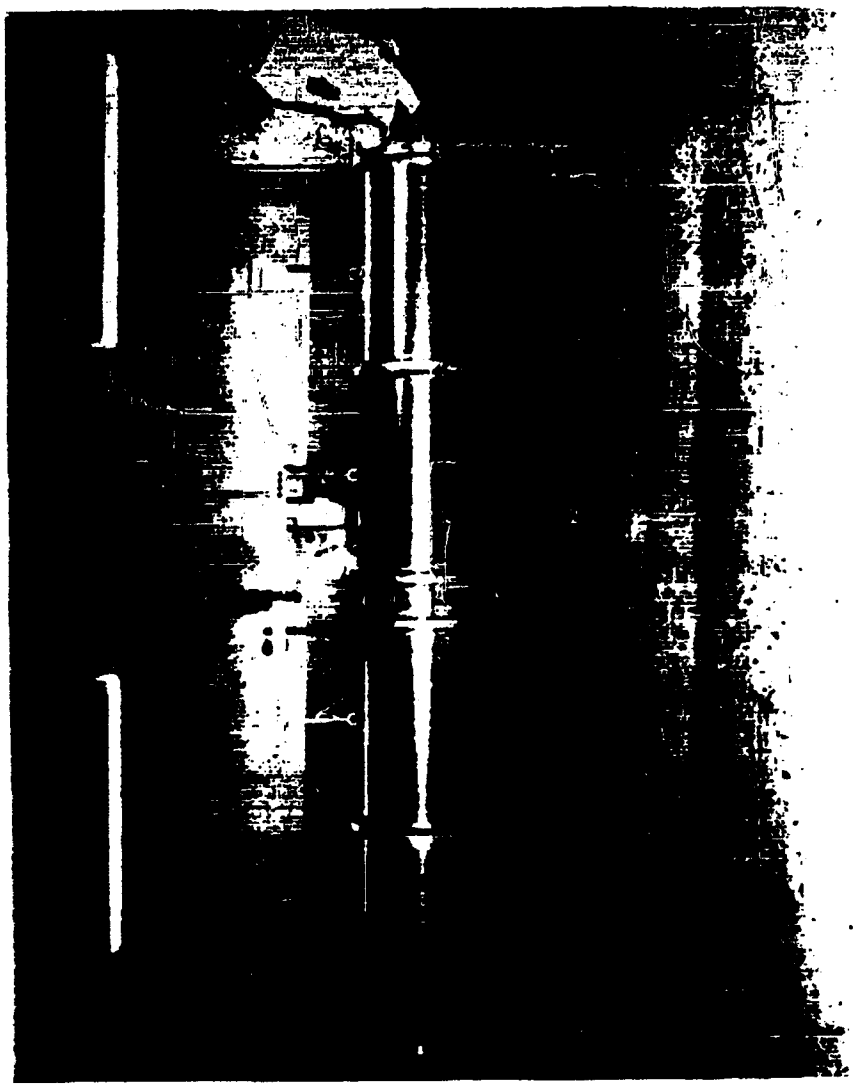

Figure 6.1 Experimental Dry-Agent Disseminator for Laboratory Design Studies

Inside diameter	18 inches
Inside length overall	117 inches
Disaggregator length	6 inches
Maximum length of each powder slug	54 inches
Maximum L/D ratio of powder slug	3
Maximum volume of powder	15.9 cu ft
Maximum weight of powder (ρ = 0.5 gm/cc)	512 lbs
Lead of piston drive screws	0.2 inches/rev
Powder feed rate	0.059 cu ft/rev
Drive speed range	8.75 to 26 rpm
Powder feed rate range	0.515 to 1.53 cfm

The cylinder is made in five sections. Four of the sections are 27.75 inches long and the center section is only six inches long. Thus, when assembled, the cylinder is 117 inches long. The disaggregator occupies the six-inch center section. The hub on each piston is 1.5 inches long leaving a maximum length of 54 inches on each end for the powder. Bearings and seals for the drive screws are mounted on the end plates of the cylinder. On one end plate the driving end of the screw protrudes through the cover of the bearing housing (see Figure 6.2). The overall exterior length of the unit is 128 inches.

The disaggregator as shown in Figure 6.3 has been removed from the center section. The assembled position is shown in Figure 6.4. The disaggregator consists of two 0.25-inch thick circular plates mounted on a hub with internal threads which engage with mating threads on the drive screws. Flat pins are used to key the hub to the drive screws. Each plate has eight rectangular openings with a cutter positioned in each opening. As the plates rotate, the cutters shave off powder which falls through the openings into the space between the plates. Baffles are mounted between the plates to stir the powder as it is mixed with gas. Wire scrapers attached to the plates are used to prevent powder from plugging the orifice or clinging to the cylinder wall.

Each piston is a 0.625-inch thick flat plate secured to a hub. Figure 6.5 shows a piston and drive screw in a cylinder (pulled out of normal position for photographic purposes). A notch in the edge of the piston

Figure 6.2 Drive End of Dissimilator

Figure 6.3 Disaggregator Removed from Center Section

Figure 6.4 Disaggregator Positioned Center Section

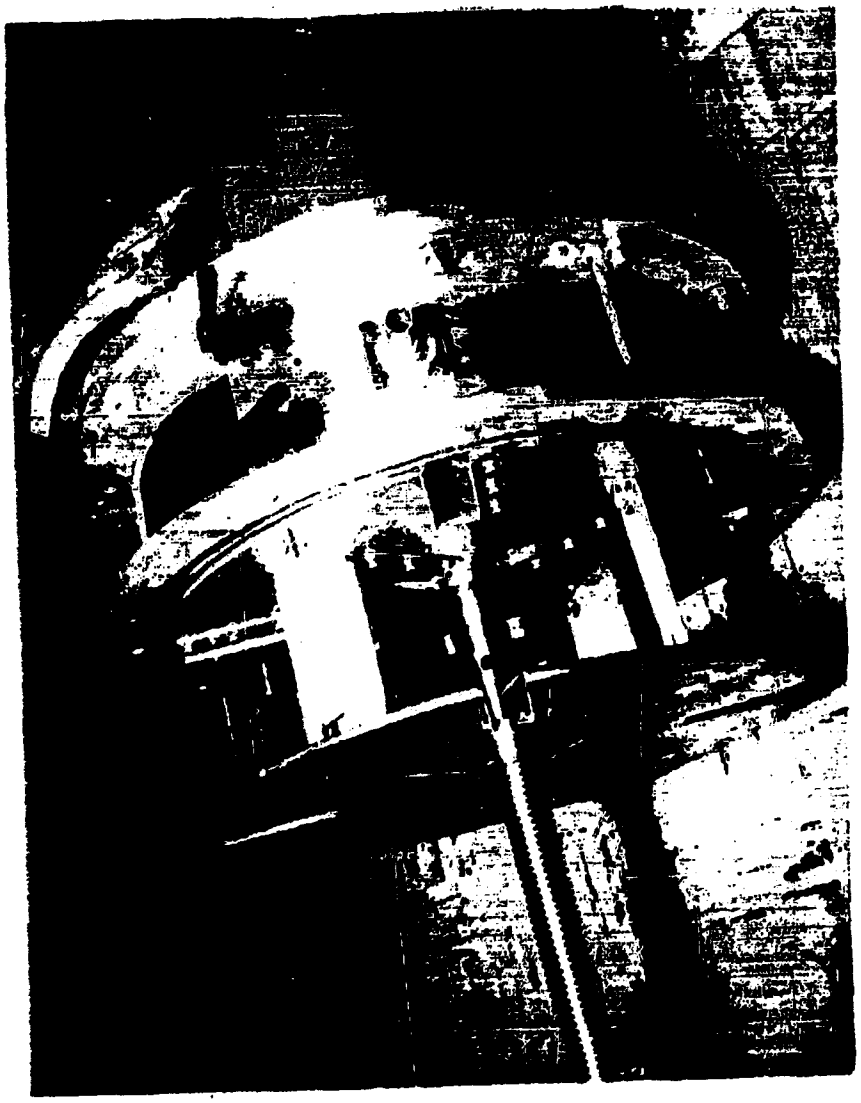

Figure 6.5 Piston and Drive Screw in Cylinder

engages with a guide running the length of the cylinder. This guide together with the frictional force of the piston against the powder prevents the piston from rotating with the screw.

Each drive screw is an Acme screw 1.375 inches in diameter with five threads per inch. A right-hand thread is used on the screw in the drive end of the cylinder and a left-hand thread on the other screw.

Figure 6.3 shows the removable plate for gaining access to the center section. The fittings for the gas supply and for pressure measurement are also evident in the photograph. (Pressure tap is partially obscured by handle or left cover latch.)

Fittings are also mounted in the end plates so that the spaces behind the pistons can be supplied with gas to balance the pressure of the gas in the center section where the powder is being fluidized.

The discharge orifice is mounted in an adapter shown in Figure 6.6 which screws into the bottom of the center section. The orifice plate is removable so that different orifice openings can be tried. Initially, orifice diameters of 3/8, 1/2 and 3/4 inches will be available for test.

6.2 Test Stand and Auxiliary Equipment

The drive for the unit consists of a 60:1 gear reductor driven by a 1.5 hp, 1750 rpm motor through a belt and a variable pitch pulley. The pulley provides a speed range of three so that the total reduction from motor to reductor shaft can be varied from approximately 60:1 to approximately 180:1 giving a theoretical reductor output speed range of 9.7 to 29.2 rpm. The output of the reductor is connected to the drive screw of the disseminator by means of a universal joint.

The test stand is designed to hold the fluidizer sufficiently high off the floor to permit collecting and weighing the powder being discharged. The powder will be collected in a large drum resting on a platform scale positioned below the disseminator.

Figure 6.6 Adapter with Discha[illegible]fice[illegible]

Provisions are being made for supplying gas from either of two sources. For the initial trials air from the plant compressed air system will be used. For tests where humidity is to be controlled and where other design conditions are to be simulated more closely, compressed nitrogen will be supplied from gas cylinders. Supply pressures will be reduced to appropriate values somewhere in the vicinity of 5 psig. Gas flow will be measured with a flow meter giving flow rate information.

A simple loading stand was designed for manually loading and compacting powder into the cylinder. The cylinder will be loaded one-half at a time by placing the cylinder half-section on end in the loading stand. A predetermined amount of powder will be placed in the cylinder and compacted with a special ram and lever arrangement. The amount of powder used per charge will occupy only a few inches in the cylinder so that it will be necessary to repeat the process several times before the half-section is filled. This is the procedure which has been used to obtain uniform density in the compacted powder when small cylinders are used.

6.3 Test Plans

It is planned that the first tests conducted with the experimental disseminator will be run with talc as the simulant material and compressed air as the gas. These first tests will be used to evaluate the basic principles involved and to make necessary modifications to the unit. In addition, data relating powder flow rates to orifice diameter, gas flow rate, gas pressure, piston feed rate, etc. will be obtained. All of this work will be conducted at room conditions without attempting to control humidity. When the unit is performing satisfactorily, a different simulant will be used and humidity will be controlled. Compressed nitrogen (and perhaps CO_2) will be used as the motivating gas. Corn starch, powdered milk or powdered sugar will be used as the simulant material. These tests will provide the data required to design the prototype airborne disseminator.

Following is a listing of data which will be obtained during the tests:

1) Material density

2) Material flow rate

3) Gas pressure

4) Gas flow rate

5) Input torque

6) Input speed

7) Humidity conditions

8) Uniformity of material flow rate

9) Other qualitative information regarding characteristics of materials or equipment which will be of value in designing the disseminator and related filling, loading, and handling equipment.

7. APPARATUS TO BE FURNISHED FOR DISSEMINATION EXPERIMENTS AT FORT DETRICK

A series of dissemination experiments will be conducted as a cooperative effort involving members of the Fort Detrick technical staff and technical personnel from General Mills, Inc. These experiments will be conducted in the large spherical ("eight ball") aerosol test chamber at Fort Detrick. The special apparatus for these experiments will be furnished by General Mills, Inc. This apparatus includes a special blow-down wind tunnel and a dissemination test fixture.

The experiments will include a series on dissemination of a dry agent simulant and also a series with an actual solid agent. The work with the simulant will provide data for comparison with our findings in the wind tunnel experiments conducted at General Mills, Inc. and with data obtained at Fort Detrick in the past. The experiments with an actual solid agent will provide necessary data on the effectiveness of the dissemination concepts currently under study.

During this reporting period, the design of the wind tunnel apparatus to be furnished to Fort Detrick has been initiated. This tunnel will be very similar to the one used in our laboratory, except for changes required to make it compatible with the "eight ball" facility and improvements suggested by our past experience. The tunnel installed in our laboratory is illustrated and described in the First Quarterly Report[15] on this project. Several detailed considerations pertaining to the design of the apparatus for the new series of experiments are discussed in the paragraphs which follow.

7.1 Safety

Special attention has been given to safety in selecting all components of the system, since some experiments will be conducted with an actual agent. In general, the system will be of welded construction. At locations where joints in the system are required for installation and handling purposes,

the flanges will be modified to incorporate an acceptable O-ring type seal. At the location where the wind tunnel is joined to the glove-box on the test sphere, a flexible coupling (metal bellows) will be provided which will maintain a tight seal and also allow for some misalignment between the two components. The entire system will be fabricated in accordance with applicable safety codes.

7.2 Air Supply for the Wind Tunnel

The blow-down system will be capable of maintaining air velocities in the test section up to Mach 0.8 for durations of 10 seconds or more. Air will be stored in three vertical cylindrical tanks approximately 30 inches in diameter and 96 inches high. These tanks will be suitable for an operating pressure of 200 psig (A.S.M.E. code) and will be equipped with an appropriate safety relief valve.

Air will be delivered to the storage tanks by oil-free two-stage reciprocating compressors. A survey of commercial compressors has been made and it was found that the most economical compressors for this application are 3/4 h.p. light-duty compressors made by Bell and Gossett Co. (Model SYCO-12-1). The capacity of these small compressors is 2.0 SCFM (measured at the inlet) with a discharge pressure of 190 psig. Several of these compressors will be installed in parallel to provide the required capacity. The use of several parallel units has the advantage of minimizing the probability of the system becoming inoperative due to compressor failure. With the tests at Fort Detrick scheduled for a short duration, this is an important advantage.

Calculations were made regarding the number of compressors required based on the time available to replace the air exhausted in a test run. With six runs per day anticipated, about one hour of pumping time is the maximum desirable period.

In the M = 0.8 tests with a duration of 10 seconds, approximately 45 pounds of air will be required. Five compressors will meet this requirement and will be furnished for this application.

With respect to the power requirement for these air compressors, it is anticipated that a total of 25 amps at 250 volts will be required.

7.3 Heat Exchanger

In the normal operation of the blow-down wind tunnel, the air in the storage tanks expands and is cooled substantially. In order to minimize temperature variations in the air passing through the test section, a storage-type heat exchanger will be provided. Calculations and experience with our previous heat exchange show that an eight-inch pipe section filled with approximately 500 pounds of small-diameter steel pipe has sufficient heat transfer effectiveness and heat capacity to limit the temperature drop to approximately 20°F below room temperature.

7.4 Stilling Chamber and Filter

A stilling chamber is important in the wind tunnel system to minimize turbulence. The stilling chamber to be used is a straight section of 8-inch diameter pipe located immediately upstream from the nozzle. This chamber will also include a screen and a filter which will contribute to the reduction of turbulence. The filter is desirable because it will collect foreign particles in the airstream. It also acts to reduce large-scale turbulence, which may be introduced in the piping, to fine-grained turbulence which readily dissipates along the length of the stilling chamber. To take advantage of this characteristic, the filter will be installed in the upstream end of the stilling chamber. It can be removed through an access flange for cleaning or replacement.

7.5 Nozzle and Test Section

The nozzle provides a smooth transition from the circular stilling chamber to the smaller rectangular test section. A molded plastic (reinforced with glass fiber) nozzle has been designed for this application.

The test section has been simplified somewhat from the design used in the wind tunnel in our laboratories. Two observation windows will be provided rather than six, and the variable area nozzle has also been eliminated since adequate control can be obtained without this feature.

The test section will be made to accept a dissemination test fixture, employing the principles currently under study on this project. This fixture will incorporate a piston-type feeder in which a total agent charge of approximately 1.0 gram will be delivered at high instantaneous mass flow rates, comparable to full-scale dissemination systems.

8. PROGRESS ON THE LIQUID DISSEMINATING STORE

As one part of the work being performed under Phase II of this contract, a liquid BW agent disseminator is being designed and fabricated. This is an external store with a liquid agent capacity of 180 gallons and a fixed flow rate of 18 gallons per minute. The configuration and operating principles of this store are described in our Fifth Quarterly Progress Report[16], which also outlines the progress on this disseminator, up to September 4, 1961.

During the present reporting period, progress has been made on the design effort and also in purchasing and fabricating parts. Sections 8.1 and 8.2 describe progress in these areas.

8.1 Design Effort

8.1.1 Design of Tank Assembly

As used here the term tank assembly includes the skin, the structure, the inner tank, the foamed-in-place insulation and the mountings and brackets for supporting the various components that are included in the finished disseminator. Prior to September 4, 1961, the general requirements for the tank assembly had been established. These general requirements included such things as the space within the outer tank, the weight of the load to be carried, the approximate location of the centers of gravity of the various loads and the external form of the tank. It was then necessary to establish the requirements in detail for the tank assembly. These details were concerned to a great extent with the provisions for mounting, supporting and containing the many system components that must be included in the finished disseminator assembly. Some examples of the items that were considered are:

1) The turbine support ring and the method of attaching the turbine to it.

2) The access doors – their size and location.

3) Bulkheads, and the provisions for attaching parts and making connections through them.

4) The method of supporting the inner tank.

5) The supports that must be provided for the fluid handling system.

6) The requirement for the insulation and its relation to the loads it bears and the conditions it must resist.

7) Required clearances for moving parts, and for assembly of parts and components into the structure.

8) The boom wells.

9) The structural requirements imposed by the many different loads applied to the structure under conditions of handling and flight.

As a result of establishing the requirements for these and other details, the design was completed. These drawings, as well as those covering the entire design will be submitted at the completion of the fabrication of the disseminator.

8.1.2 Design of the Fluid Handling System

During this reporting period the design layout for the fluid handling system was completed. Requirements for the specific components were established. These requirements include such items as the flow capacities for tubes, fittings, valves and hoses; the allowable pressure losses in all parts through which liquid flows; and the pressure required of the pump. Requirements for other characteristics such as leakage, corrosion resistance, temperature resistance, formability and method of assembly were established. Additional restrictions were imposed by the limited space

available and the need for keeping the weight to a minimum. With these requirements established, it was possible to select the major purchased components in the fluid handling system such as valves, the flow indicator, the pump and also the tubing and fittings.

8.1.3 Design of the Electrical System

One of the design objectives of the project is to make the disseminator compatible with the F-100D aircraft. In order to achieve this, it was necessary to determine the detailed characteristics of the electrical system in this aircraft. For this purpose, General Mills, Inc. personnel visited McClellan Air Force Base near Sacramento, California, to discuss the electrical system with Air Force personnel. As a result of this meeting, a system was designed that is compatible with this aircraft. That portion of the system for which the compatibility requirement exists includes control of the power supply, lowering and raising of the booms, control of the pump and the transmitting of flow signals to the pilot.

Design requirements were also established for operating the system using either ground-power or air-turbine-power for operation of the system.

An important element in the system is the control box and panel that the pilot uses for operating the disseminator. While our personnel were at McClellan Air Force Base, they determined what space was available for a control box and the necessary mounting provisions. The disseminator control unit will occupy the space normally used for control of the "buddy" refueling system.

Based on the requirements outlined above, and on the selection of suitable electrical components, the control system circuits were laid out and the design of the control box and panel was initiated.

8.1.4 Design of the Booms and Boom Actuator

Design work on the booms and the boom actuator was continued. The mock-up referred to in the Fifth Quarterly Report[16] was completed. It demonstrates that the actuating system will operate satisfactorily within the available space in the tail section.

Work was continued on the fabrication of nozzle slits. The method finally accepted was the ultrasonic grinding technique. By selecting the proper tool size, the right grit size and maintaining the necessary control of other variables, a process was established that provides good control of slit dimensions. The boom nozzle slits are to be 0.400 inches in length and 0.0048 inches wide, nominally. These dimensions were established as a result of the experimental work done in making slits and also as a result of flow tests conducted with tubes containing from one to nine slits.

The ultrasonic grinding technique was selected in preference to the spark erosion method and chemical etching process which were also investigated. Both of these methods failed to produce slits having straight edges.

Analyses of the boom assembly as a structure was continued. This included calculation of the stresses resulting from the aerodynamic loading and also a study of the vibration characteristics.

Further study was also made of the heat transfer characteristics and the heating requirements. As a result of this study, the areas which are to be coated with Electrofilm heaters were determined.

The decision was made to protect the booms in the boom wells by covering the wells with Mylar film, taped to the tank skin. The booms have knife edges on them that cut through the Mylar as the booms are lowered. The Mylar film cover must be replaced (by a simple operation) before re-use.

8.2 Purchasing and Fabrication of Parts

As a result of the design effort described above, it was possible to place orders for all of the major purchased parts during this reporting period. The major parts ordered included the reinforced plastic inner tank, the main tank assembly (skin structure, etc.), the air turbine generator, the flow indicator, the various fluid-system valves, the boom actuator, and numerous other parts including relays, wire, tubing, thermostats, fittings and fasteners. Of the major items ordered, the reinforced plastic inner tank was received at General Mills, Inc. and the remainder are to be delivered during December and January.

It is anticipated that the main tank assembly (with the inner tank foamed-in-place) will be received from Fletcher Aviation Co. by December 15, 1961, permitting installation of the other components thereafter.

9. SYSTEMS STUDY

A continuing BW dissemination systems study has been underway on this contract. In our Fourth Quarterly Progress Report[17], a mathematical model was introduced which has been used in this study since that time. This model is a modification of the one attributed to K. Calder. The modification deals with variable rates of decay of the agent versus time.

During this reporting period, the model has been applied to the determination of the agent flow rates (versus down-wind distance) required for a fixed injection probability. Two solid BW agents, LE and N, have been selected for the calculations performed during this period. Since the required flow rate depends on many factors including meteorological parameters, height and speed of the delivery aircraft, efficiency of dissemination, and efficiency of particle retention by man, we have investigated several specific cases.

In the analysis which follows, the nomenclature is the same as used previously. Table 9.1 defines this nomenclature.

Table 9.1 Nomenclature

Symbol	Definition
b	Breathing rate of a man
C	Agent concentration
d	Agent dosage per person
D_L	Ground level dosage of the agent
E	Dissemination efficiency
E_r	Efficiency of retention of particles with "size" r
$\bar{E}_r$	Mean efficiency of retention
erfc(x)	Complementary error function $\int_x^\infty \exp(-\xi^2/2)\, d\xi$

Table 9.1 (Continued)

Symbol	Definition
f	Dissemination flow rate
h	Height of an aircraft
h_a	Adjusted height of release
ID_{50}	Number of organisms required to infect 50% of the people
k	Agent decay
L	Half of length of release line
ℓ	Distance along the aircraft path
P	Probability of infection
q	Source strength
r	Particle "size"
t	Time after release
u	Wind speed
v	Aircraft speed
σ	Weather parameter
β	Weather parameter
x_1	Height for which σ and β are determined

In addition to previous analyses, equations have been written describing the decay process for the agents LE and N. The data for 30 percent relative humidity given in Reference 18 are approximated by the equations below:

For the agent LE, the "decay factor" is:

$$3.75 \left(\frac{x}{u}\right) \Big/ \left(\frac{x}{u} + 1\right)^{1.59} \qquad (9.1)$$

For the agent, N, the "decay factor" is:

$$0.0985 \left(\frac{x}{u}\right) \Big/ \left(\frac{x}{u} + 1\right)^{1.93} \qquad (9.2)$$

The equation relating the total dosage, d, and the probability of infection, P, is

$$P = 1 - \exp\left[- \frac{d}{\text{---}_{50}} \right] \qquad (9.3)$$

where the dosage for an infinite instantaneous line source is related to other parameters by

$$d = \sqrt{\frac{2}{\pi}} \; \frac{bf\, EC\, \overline{E}_r}{v\, \sigma_3\, u\, (x/x_1)^{\beta}} \; \exp\left[- h_a^2 \Big/ 2\sigma_3^2 \, (x/x_1)^{2\beta} \right] \exp\left[- \text{decay factor} \right] \qquad (9.4)$$

In the previous analyses, probability of infection was plotted as a function of down-wind cloud travel for different values of the parameters. A typical plot is shown in Figure 9.1. For a fixed probability, say P_o, the region enclosed by lines $x = x_1$ and $x = x_2$ and also the region near the release line have the probability of infection greater than P_o while everywhere else it is less. We can say then, that these regions will have an effective coverage for a certain flow rate, i.e., for a preselected infection probability, P_o, an appropriate flow rate can be determined such that the region will be effectively covered. It is this aspect of the analysis that we wish to consider presently.

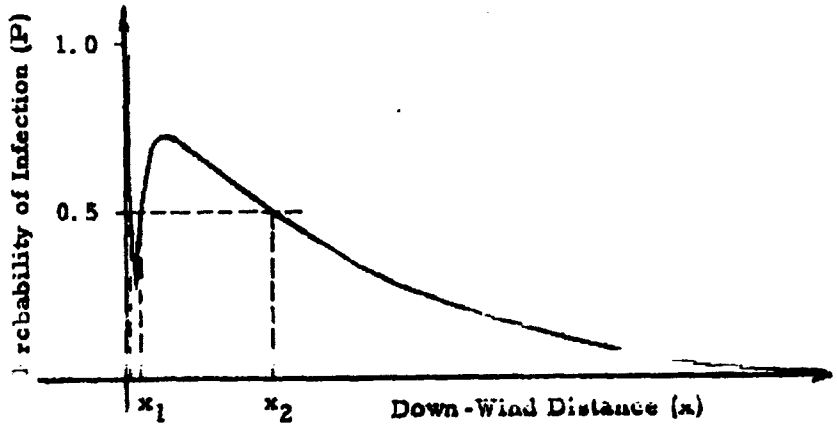

Figure 9.1 A Typical Curve for Probability of Infection versus Down-Wind Distance

A typical graph for present study is shown in Figure 9.2. Here the flow rate versus the down-wind distance is plotted for a fixed probability, say P_o. It is clear that a constant flow rate corresponding to x_2 will guarantee an infection probability of at least P_o for the entire region. If only a portion of the region for $x < x_1$ (for example) is to have an infection probability of at least P_o, then the flow rate to be used must correspond to x_1 of the curve. The region extending beyond this will have a lower value of P for the same flow rate. It is assumed that the release line is long enough so that the contamination is uniform, crosswind, for a fixed distance from the source.

Based upon the diffusion depostion model presented above, a set of curves were drawn by the Bendix PA-3 plotter, coupled with the Bendix G-15D digital computer. For all the curves, the infection probability, $P = 0.5$; efficiency of particle retention, $E_1 = 0.33$; efficiency of dissemination, $E = 0.20$; speed of the aircraft, $v = 545$ mph; and breathing rate of a

man, b = 25.4 ft^3/hr. The concentration-to-infective-dose ratio, $C/ID_{50} = 1.67 \times 10^7\ ml^{-1}$ for agent LE and $C/ID_{50} = 1.25 \times 10^8\ ml^{-1}$ for agent N. The last two values are estimates. In connection with biological decay, Equations (9.1) and (9.2) must be considered as approximations only due to limited availability of data. The weather conditions defined arbitrarily by other investigators[19] as "good" and "average" refer to values of σ_3 and β as $\sigma_3 = 12.47$ feet, $\beta = 0.66$ and $\sigma_3 = 19.03$ feet, $\beta = 0.88$, respectively with $x_1 = 300$ feet for both cases. The curves are presented in Figures 9.3 through 9.8.

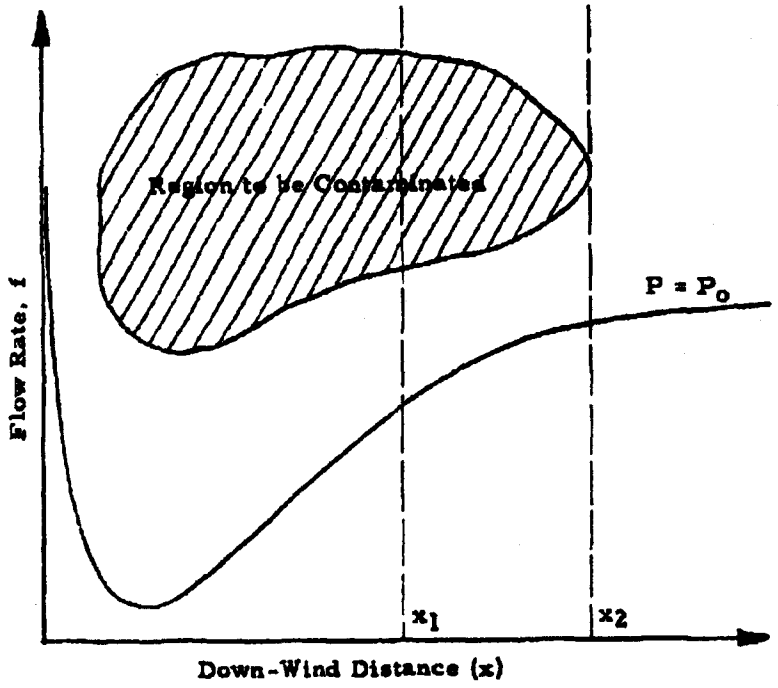

Figure 9.2 A Typical Curve for Flow Rate versus Down-Wind Distance (x)

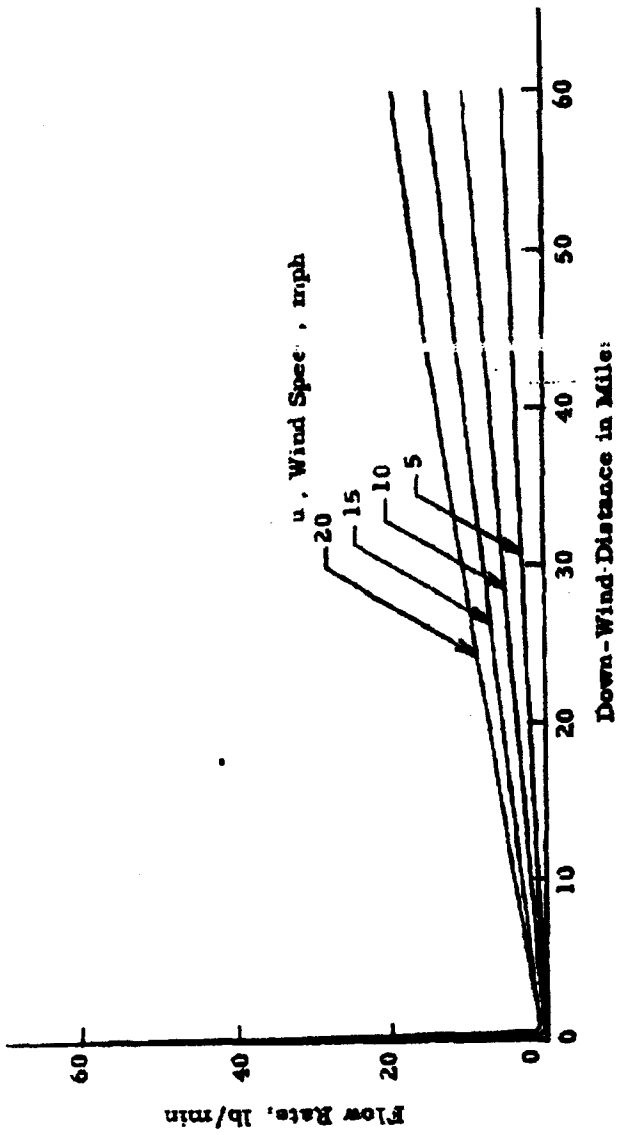

Figure 9.3 Flow Rate versus Down-Wind Distance for Agent N for "Average" Weather and h_a = 5 feet

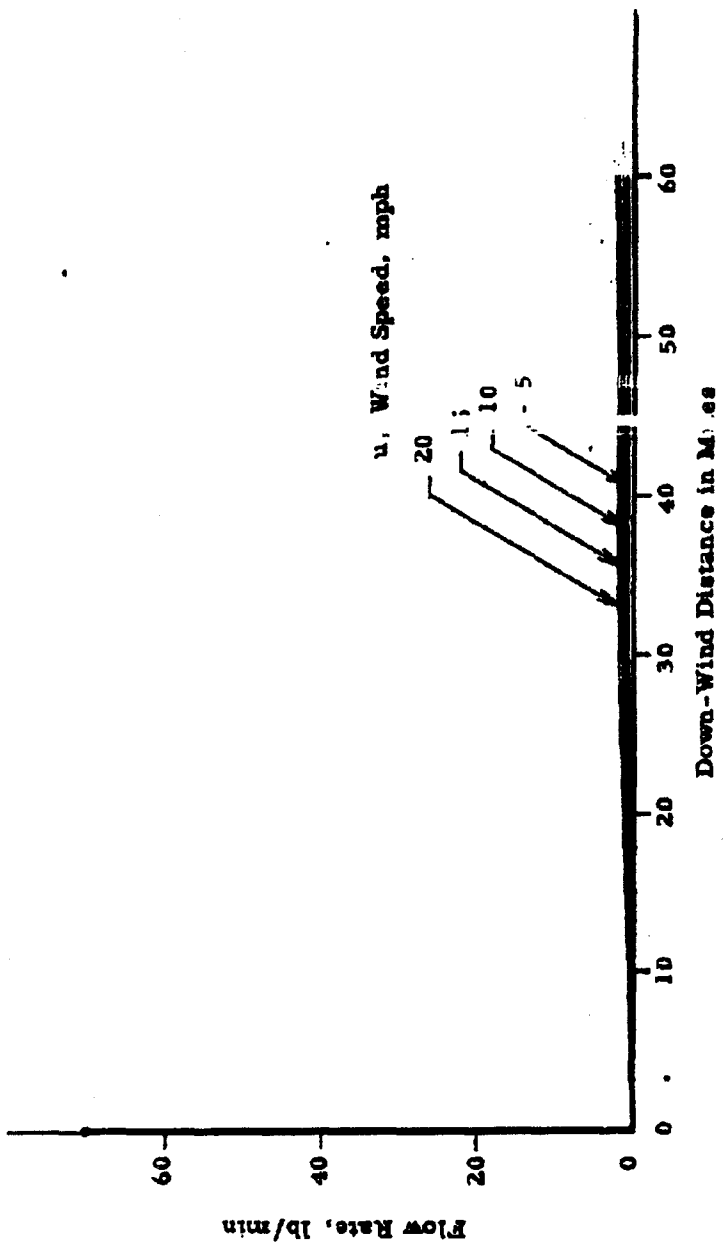

Figure 9.4 Flow Rate versus Down-Wind Distance for Agent N for "Good" Weather and h_a = 55 feet

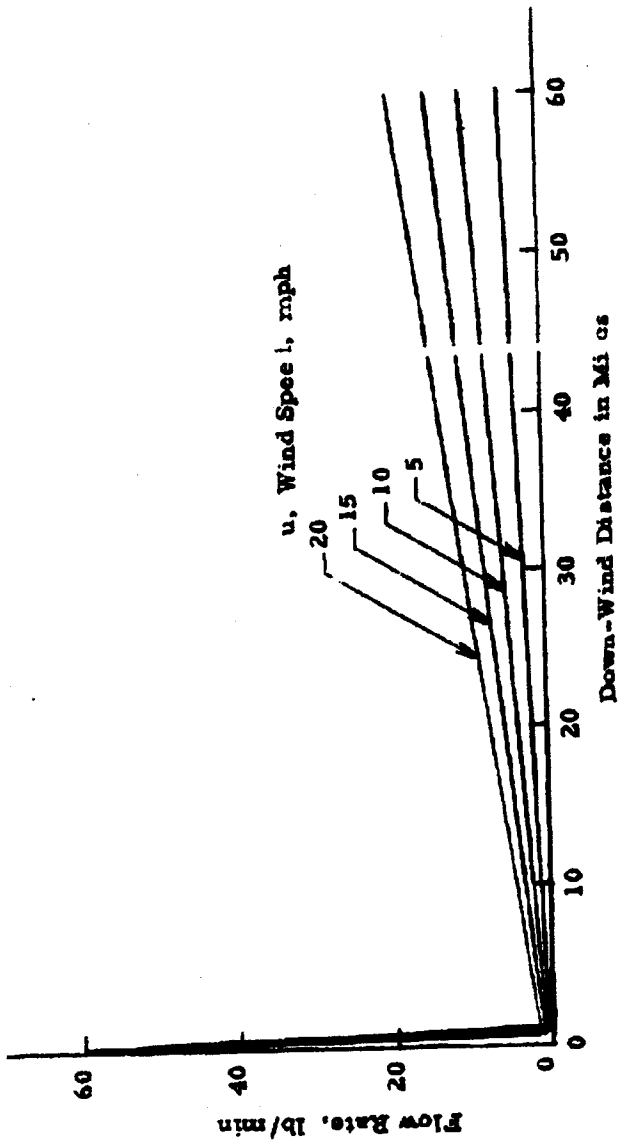

Figure 9.5 Flow Rate versus Down-Wind Distance for Agent N for "Average" Weather and h_s = 100 feet

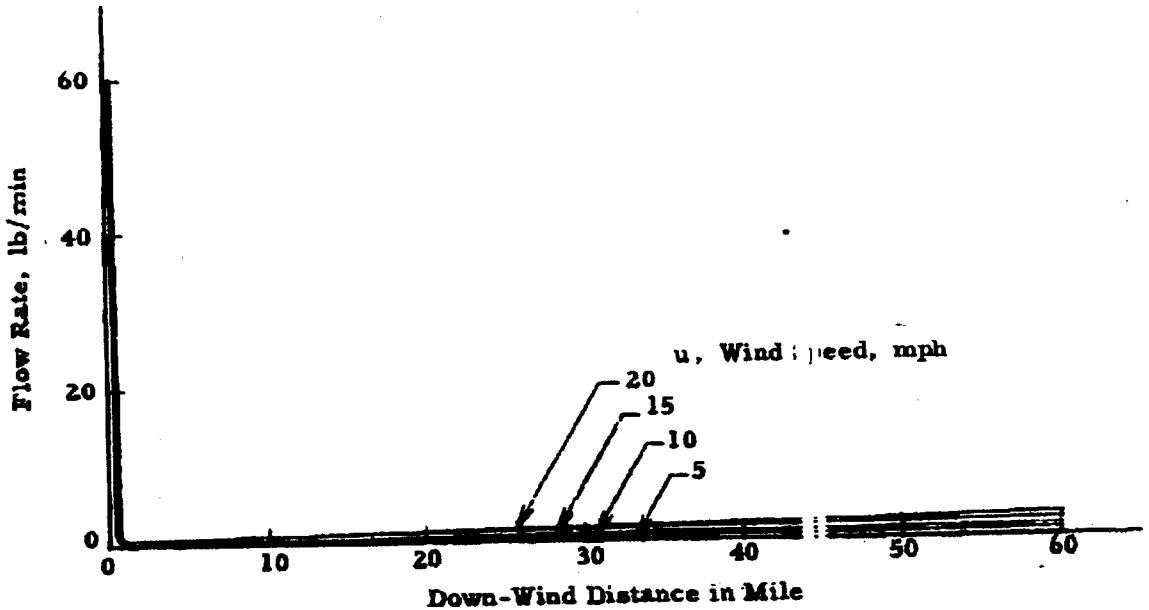

Figure 9.6 Flow Rate-versus Down-Wind Distance for Agent N for "Good" Weather and h_s = 100 fe

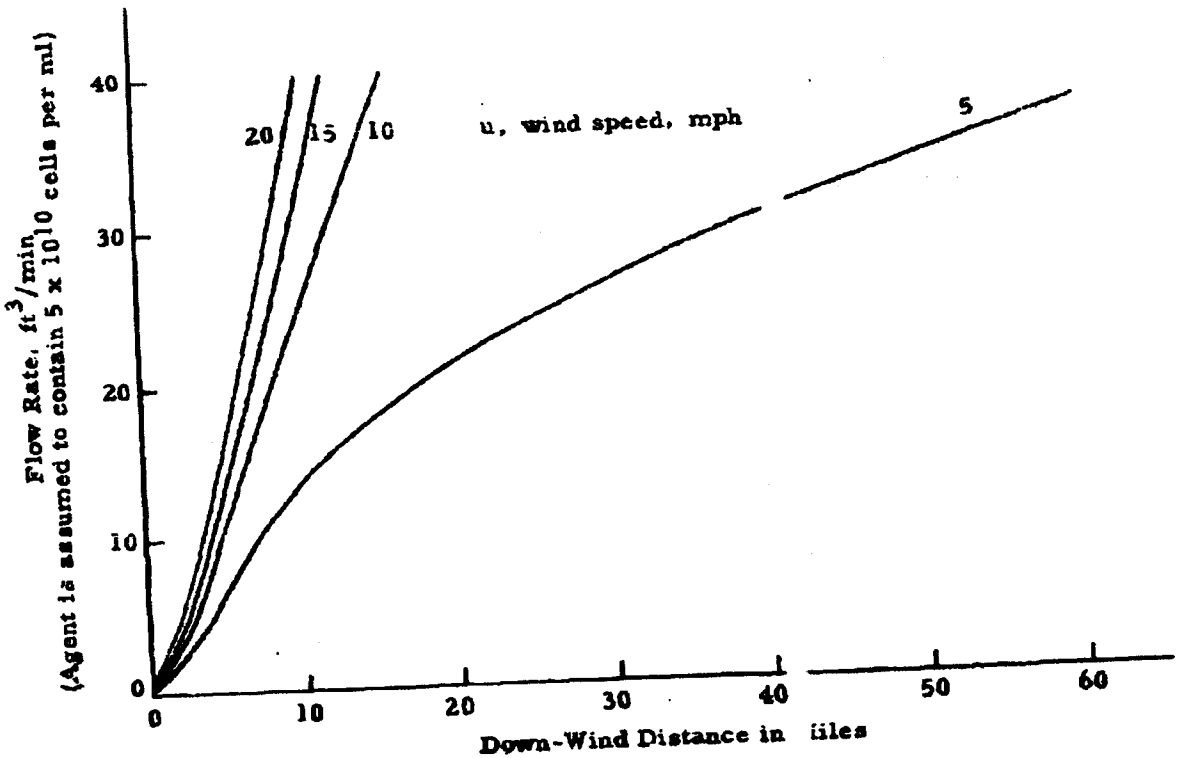

Figure 9.7 Flow Rate versus Down-Wind Distance for Agent LE for "Average" Weather and h = 55 feet

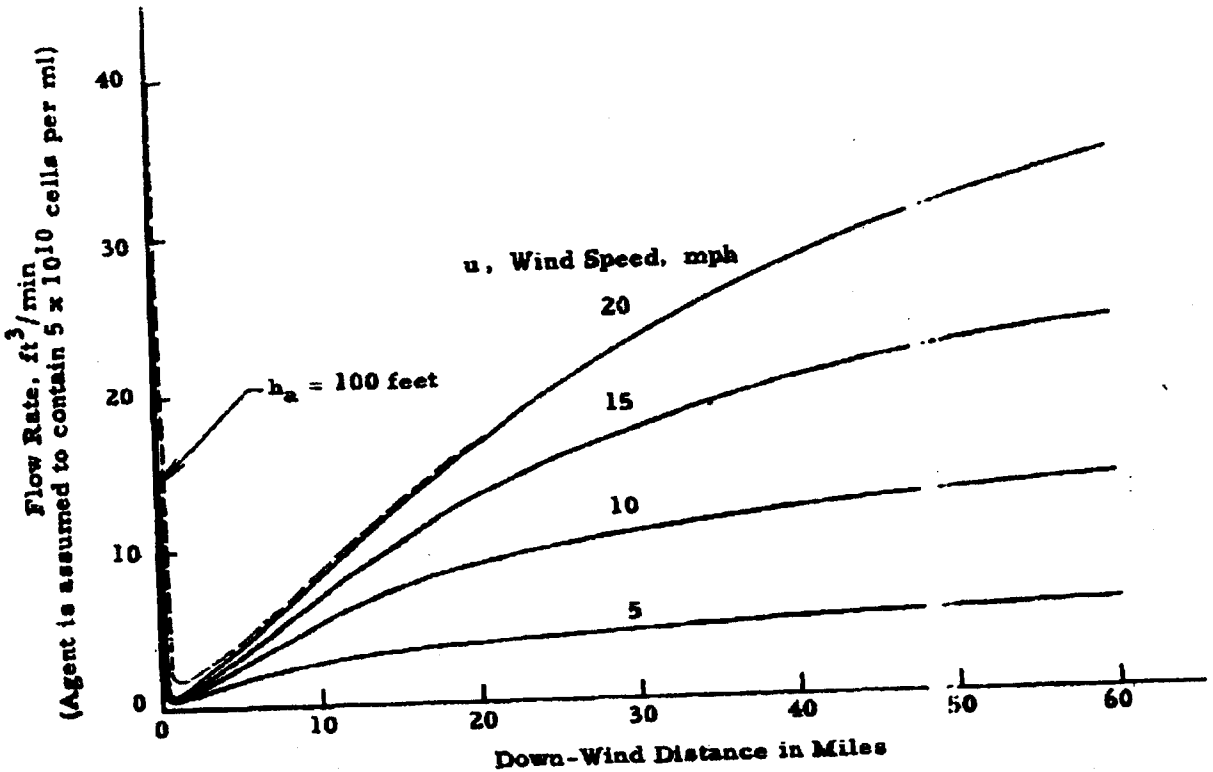

Figure 9.8 Flow Rate versus Down-Wind Distance for Agent LE for "Good" Weather and h_a = 55 feet (and 100 feet)

It is noted by comparing Figure 9.3 with Figure 9.5 and Figure 9.4 with Figure 9.6, all of which pertain to the agent N, that the flow rate is affected very little when the source elevation is nearly doubled. This comparison is shown in Figure 9.8 for the agent LE where the flow rate for aircraft heights of 55 feet and 100 feet are compared. Near the source there is some deviation between the two curves, but this diminishes with increasing down-wind distance. In all the graphs the flow rate is infinity at the source, as is to be expected from the diffusion model adopted. The minimum value of this flow rate is assumed for x satisfying the equation:

$$k^1 x^2 + kx - \frac{\beta h^2 u}{\sigma_3^2 / x_1^{2\beta}} x^{-2\beta} + \beta u = 0. \qquad (9.5)$$

For the cases considered, the above equation has a root for $x < 1.5$ miles, as is seen from the graphs. At approximately this distance, then, the probability of infection will be highest for a selected flow rate.

Figures 9.3 through 9.6 show that effective coverage over very large areas can be achieved with low to moderate flow rates of the solid agent N. The low decay rate of this agent is an important factor in this connection.

For agent LE (see Figures 9.7 and 9.8) note that the flow rates are specified in ft^3/min. This change in units (from lb/min in Figures 9.3 through 9.6) was considered necessary because the concentration of the agent was known on a volumetric basis and density was not available. The agent LE requires very high flow rates, except for cases involving distances below five miles for good weather and approximately two miles for average weather.

To date, the solid agent UL, which is of considerable interest, has not been studied because the data relative to decay at extended time periods are not available. We believe that additional basic research in this area would be very valuable.

10. SUMMARY AND CONCLUSIONS

During this reporting period substantial progress was made in several of the important areas of investigation concerned with the problems involved in dissemination of solid BW agents. Also, the effort devoted to design and fabrication of a liquid BW agent dissemination store has provided good results. Progress on the several activities is summarized below, in the order the topics appear in the main body of this report.

In connection with the theoretical study of the mechanics of particulate materials, the investigations of the process of compaction of dry powders have been continued. Careful examination has shown that the compaction process is very complex and that the energy spent in compaction may appear as 1) an increase in potential energy associated with interparticle bonds, 2) stored elastic energy in the bulk powder, and 3) thermal energy which is dissipated in the process. To further explore the energy distribution in this process, three types of experiments have been devised and apparatus is being developed to conduct these experiments. Additional experiments with current apparatus have shown that the net work of compaction is related (for talc, saccharin, Sm and cornstarch) to the bulk density by an exponential equation (Section 2).

The experimental measurements of the physical characters of powders have been continued. Extensive work has been done on investigation of powder shear strength as a function of compressure stress, moisture content and bulk density. One of the most interesting findings was that the shear strength of the talc powder increases very rapidly when compacted to bulk densities above 0.4 gm/cm^3. Upon closer examination, it was found that the shear strength is an exponential function of the bulk density. The measurements of the force required to move a powder plug through a cylinder with a piston were extended to cover pre-compacted powders. It was found that the ratio of applied force to resistive force was identical to that required to move an uncompacted plug of the same length, as long as the resistive force was above some critical value. If the resistive force was less than the critical value, a new relationship exists (Section 3).

Experimental studies of the effect of elevated airstream temperatures on the viability of dry aerosols of Bg and Sm were continued. The recovery of viable organisms was determined over the range of temperatures between 30°C and 130°C. It was found that exposure of dry Bg for a period of 1.68 seconds had no measurable effect on the viability. In contrast, there was a pronounced viability loss with Sm upon exposure to airstreams between 75°C and 130°C for periods of 1.12 and 1.68 seconds (Section 4).

The wind tunnel studies of deagglomeration by slipstream energy have been continued, with emphasis on determination of the number and mass of agglomerates in the generated aerosol. The deagglomeration studies during this period have shown that compacted Sm with bulk densities as high as 0.65 gm/cm^3 can be disseminated with a mechanical-pneumatic system nearly as effectively as the uncompacted material. The results indicate that the maximum loss in effectiveness due to agglomeration of particles in the 1 to 5-micron range is approximately 12 percent by mass (Section 5).

With respect to the investigations of feeding systems for dry agent disseminators, a full-scale laboratory unit was designed and fabricated. This unit is based on the operating principles we have advanced for an airborne dry-agent disseminator. Test plans have been established for future work with this experimental model (Section 6).

The design effort on apparatus to be furnished to Fort Detrick was initiated during this period and good progress was made. A blow-down wind tunnel quite similar to the one used by General Mills, Inc. will be installed at the "eight-ball" test sphere facility for use in dissemination experiments (Section 7).

Considerable progress was made during this reporting period on the design and fabrication of the airborne liquid BW agent disseminator. Detailed requirements for the overall unit and its many components were established. Orders were placed for all of the major purchased components of the store. Delivery of the reinforced plastic inner (agent container) tank was received (Section 8).

The systems studies were continued, with specific cases being evaluated using the variable-decay mathematical model. Line source dissemination of agents LE and N were studied. Plots of flow rate versus down-wind travel are given (Section 9).

11. REFERENCES

1) General Mills, Inc. Report No. 2249, Fifth Quarterly Progress Report on Dissemination of Solid and Liquid BW Agents (Unclassified Title), November 30, 1961 (Confidential), p. 8.

2) General Mills, Inc. Report No. 2249, Fifth Quarterly Progress Report on Dissemination of Solid and Liquid BW Agents (Unclassified Title), November 30, 1961 (Confidential), pp. 17-24.

3) Flosdorf and Webster. J. Biological Chemistry 121:353 (1937).

4) General Mills, Inc. Report No. 2229, Fifth Quarterly Progress Report on Fundamental Studies of the Dispersibility of Powdered Materials, Contract No. DA-18-108-405-CML-824, September 30, 1961, pp. 3-9.

5) General Mills, Inc. Report No. 2200, Third Quarterly Progress Report on Dissemination of Solid and Liquid BW Agents (Unclassified Title), May 15, 1961 (Confidential), p. 15.

6) General Mills, Inc. Report No. 2161, Second Quarterly Progress Report on Dissemination of Solid and Liquid BW Agents (Unclassified Title), February 13, 1961 (Confidential), pp. 2-13.

7) General Mills, Inc. Report No. 2216, Fourth Quarterly Progress Report on Dissemination of Solid and Liquid BW Agents (Unclassified Title), August 10, 1961 (Confidential), p. 18.

8) General Mills, Inc. Report No. 2216, Fourth Quarterly Progress Report on Dissemination of Solid and Liquid BW Agents (Unclassified Title), August 10, 1961 (Confidential), pp. 2-9.

9) General Mills, Inc. Report No. 2249, Fifth Quarterly Progress Report on Dissemination of Solid and Liquid BW Agents (Unclassified Title), November 30, 1961 (Confidential), pp. 47-51.

10) General Mills, Inc. Report No. 2216, Fourth Quarterly Progress Report on Dissemination of Solid and Liquid BW Agents (Unclassified Title), August 10, 1961 (Confidential), pp. 101-103.

11) General Mills, Inc. Report No. 2216, Fourth Quarterly Progress Report on Dissemination of Solid and Liquid BW Agents (Unclassified Title), August 10, 1961 (Confidential), p. 73.

12) General Mills, Inc. Report No. 2249, Fifth Quarterly Progress Report on Dissemination of Solid and Liquid BW Agents (Unclassified Title), November 30, 1961 (Confidential), p. 28.

13) Rans, W.E., and J.B. Wang, "Impaction of Dust and Smoke Particles on Surface and Body Collectors", Industrial and Engineering Chemistry, vol. 44, 1952, p. 1377.

14) General Mills, Inc. Report No. 2249, Fifth Quarterly Progress Report on Dissemination of Solid and Liquid BW Agents (Unclassified Title), November 30, 1961 (Confidential), pp. 33-46.

15) General Mills, Inc. Report No. 2125, "Dissemination of Solid and Liquid BW Agents" (Unclassified Title), October 13, 1960 (Secret), pp. 21-25.

16) General Mills, Inc. Report No. 2249, Fifth Quarterly Progress Report on Dissemination of Solid and Liquid BW Agents (Unclassified Title), November 30, 1961 (Confidential), pp. 59-68.

17) General Mills, Inc. Report No. 2216, Fourth Quarterly Progress Report on Dissemination of Solid and Liquid BW Agents (Unclassified Title), August 10, 1961 (Confidential), pp. 104-109.

18) Fort Detrick Report No. 61-FDS-392, "Biological Warfare Agents II, Agent Characteristics", April 1, 1961 (Secret).

19) North American Aviation, Inc. Report No. NA-59-632, "Airborne Biological Warfare at Low Altitudes", Vol. II, June 16, 1959 (Secret).